https://doi.org/10.5194/acp-2021-61
Preprint. Discussion started: 22 January 2021

Atmospheric Chemistry and Physics Discussions

SO_2 and NH_3 emissions enhance organosulfur compounds and fine particles formation from the photooxidation of a typical aromatic hydrocarbon

Zhaomin Yang[1], Li Xu[1], Narcisse T. Tsona[1], Jianlong Li[1], Xin Luo[2], Lin Du[1]

[1]Environment Research Institute, Shandong University, Qingdao, 266237, China
[2]Technology Center of Qingdao Customs, Qingdao, 266003, China

Correspondence to: Lin Du (lindu@sdu.edu.cn)

Abstract. Although atmospheric SO_2 and NH_3 levels can affect secondary aerosol formation, the influenced extent of their impact and their detailed driving mechanisms are not well understood. The focus of the present study is to examine the chemical compositions and formation mechanisms of secondary organic aerosols (SOA) from 1,2,4-trimethylbenzene (TMB) photooxidation influenced by SO_2 and/or NH_3. Here, we showed that SO_2 emission could considerably enhance aerosol particle formation due to SO_2-induced sulfates generation and acid-catalyzed heterogeneous reaction. Orbitrap mass spectrometry (MS) measurements revealed the generation of not only typical TMB products but also hitherto unidentified organosulfates (OSs) in SO_2-added experiments. The OSs designated as unknown origin in earlier field measurements were also detected in TMB SOA, indicating that atmospheric OSs might be also originated from TMB photooxidation. For NH_3-involved experiments, results demonstrated a positive correlation between NH_3 levels and particle volume as well as number concentrations. The effects of NH_3 on SOA composition was slight under SO_2-free conditions but stronger in the presence of SO_2. A series of multifunctional products with carbonyl, alcohols, and nitrate functional groups were tentatively characterized in NH_3-involved experiments based on infrared spectra and HRMS analysis. Plausible formation pathways were proposed for detected products in the particle-phase. The volatility distributions of products, estimated using parameterization methods, suggested that the detected products gradually condense onto the nucleation particles to contribute to aerosol formation and growth. Our results suggest that strict control of SO_2 and NH_3 emissions might remarkably reduce organosulfates and secondary aerosol burden in the atmosphere. Updating the aromatic oxidation mechanism in models could result in more accurate treatment of particles formation for urban regions with considerable SO_2, NH_3, and aromatics emissions.

https://doi.org/10.5194/acp-2021-61
Preprint. Discussion started: 22 January 2021


Atmospheric Chemistry and Physics Discussions

1 Introduction

Secondary organic and inorganic aerosols have been observed to account for a considerable fraction of fine particulate matter (aerosol particles ≤ 2.5 μm in aerodynamic diameter, $PM_{2.5}$) during $PM_{2.5}$ pollution events, which had frequently occurred and lasted for days or even weeks in China during the last decade (Huang et al., 2014; Guo et al., 2014). These particles can directly and indirectly impact regional and global climate (Kanakidou et al., 2005), air quality (Zhang et al., 2015), and human health (Lelieveld et al., 2015).

Secondary organic aerosols (SOA) arise predominantly from the oxidation of volatile organic compounds (VOCs) in the atmosphere. Early atmospheric models underestimated the measured SOA mass concentrations in field studies by 1–2 orders of magnitude (Volkamer et al., 2006; Heald et al., 2010). Although recent efforts such as updating missing SOA precursors, accounting unknown processes of gas-to-particle conversion, and improving emission inventories have narrowed the observed gap between the modeled and measured SOA mass, uncertainties still exist in organic aerosol estimates (Shrivastava et al., 2011; Cheng et al., 2021). Inorganic perturbations on SOA formation (Shrivastava et al., 2017) are partly responsible for these uncertainties, and they include the addition of mineral particles (Yu and Jang, 2019), nitrogen oxide (NO_x) (Zhao et al., 2018), ammonia (NH_3) (Hao et al., 2020), and sulfur dioxide (SO_2) (Yang et al., 2020), which can engage in the gas- and particle-phase chemistry and subsequently influence SOA formation and growth (Friedman et al., 2016; Ng et al., 2007; Na et al., 2006). NO_x effects on particle formation are generally known to be pronounced. High levels of SO_2, NH_3, and VOCs have been reported in certain regions (Warner et al., 2017; Zou et al., 2015), yet less focus has been placed on the SO_2 and NH_3 perturbations on SOA formation. Previous laboratory studies examined the photooxidation of cyclohexene, fuel, and 1,3,5-trimethylbenzene in the presence of SO_2 and reported organosulfates (OSs) formation (Yang et al., 2020; Liu et al., 2017; Blair et al., 2017). The atmospheric oxidation of SO_2 can generate sulfuric acid that is critical for new particle formation and the increase of particle acidity. SO_2-induced acidic sulfate plays an active role in the production of OSs, which have been recognized as significant SOA tracers describing the enhancement in SOA by SO_2 emission (Xu et al., 2015).

OSs are ubiquitous in ambient aerosol particles and they are estimated to account for 3–30% of the organic mass in fine aerosol particles (Surratt et al., 2008; Tolocka and Turpin, 2012). With highly oxygenated and sulfated molecular structure, the presence of OSs can remarkably alter aerosol morphology, viscosity, phase state, and hygroscopicity, thereby resulting in lager climate effect. A large amount of OSs has previously been observed in field measurements but

https://doi.org/10.5194/acp-2021-61
Preprint. Discussion started: 22 January 2021


Atmospheric Chemistry and Physics Discussions

only a few biogenic VOCs can be clearly designated as OSs precursors (Wang et al., 2019b; Shalamzari et al., 2014). Recent field studies reported that some unidentified OSs with C_2–C_{25} skeletons are equivocally not originated from biogenic VOCs and suggested that anthropogenic VOCs might contribute to these OSs formation (Wang et al., 2016; Blair et al., 2017). In addition, Ma et al. (2014) demonstrated that OSs derived from aromatic hydrocarbons contribute to up to 67% of the total OSs mass in Shanghai, highlighting the potentially significant role of aromatics in organosulfates formation. While several studies have shown that SO_2 emissions have implications for the SOA burden and OSs formation, detailed characterization of OSs formation from anthropogenic monocyclic aromatics photooxidation are poorly performed.

Ammonia (NH_3) is the most abundant form of reduced nitrogen and it is ubiquitous in the ambient environment. NH_3 levels increased substantially in agricultural regions in recent years and are estimated to continue to increase in the future (Warner et al., 2017). It is established that the increased NH_3 emissions could reduce the effectiveness of $PM_{2.5}$ control by controlling SO_2 and NO_x (Wu et al., 2016; Fu et al., 2017). However, the effects of NH_3 on the formation of aerosol particles have not been well understood. NH_3 has a promoting effect on the formation of new particles (Wang et al., 2020a) where low volatile organic compounds could condense to form SOA in the atmosphere. A previous chamber study reported that the addition of NH_3 could lead to the enhancement in the volume and number concentrations of SOA from α-pinene ozone system (Na et al., 2007). Another study by Babar et al. (2017) utilized newly developed flow reactor and confirmed that the presence of NH_3 can enhance SOA formation from both ozonolysis and photooxidation of α-pinene. Beside α-pinene, the promoting effects of NH_3 on particle formation were also discovered in the photooxidation of aromatics (Chu et al., 2016) and vehicle exhaust (Chen et al., 2019). In contrast, addition of NH_3 decreased aerosol particles formation from the reaction of styrene with ozone owing to the decomposition of products via NH_3 nucleophilic attack (Na et al., 2006). Laboratory evidence suggests that NH_3 can also influence SOA composition via the neutralization of organic acids (Hao et al., 2020) and via the NH_3 uptake by carbonyl-containing compounds (Flores et al., 2014). The reaction of organic compounds in particle-phase with NH_3 can decrease gaseous NH_3 concentrations and can enhance the formation of nitrogen-containing organic compounds (Liu et al., 2015), which are a class of brown carbon and thus modify SOA optical properties. The neglect of NH_3 effects on SOA formation might increase the model-measurement disagreement in SOA mass and can lead to an overprediction of NH_3 concentration in the gas-phase, especially in a complex urban environment. Consequently, it is necessary to explicitly explore the influence of NH_3 on aerosol particles formation.

https://doi.org/10.5194/acp-2021-61
Preprint. Discussion started: 22 January 2021


Atmospheric Chemistry and Physics Discussions

The complex mixture of ozone and fine particles is an emerging environmental problem affecting regional and urban air quality in China (Song et al., 2017), and investigating the chemistry of aromatic hydrocarbons has become greatly important for ozone and $PM_{2.5}$ control because aromatics have high ozone- and SOA-forming potential (Chu et al., 2020). Aromatic hydrocarbons comprise a substantial fraction of the total VOCs at urban locations and even in rural areas (Guo et al., 2006; Ran et al., 2009), and evidence shows that global SOA formation from aromatic hydrocarbons lies in the range of 2 to 12 Tg yr^{-1} (Henze et al., 2008). 1,2,4-Trimethylbenene (TMB) is a small monocyclic aromatic emitted primarily from automobiles and industrial solvent evaporation (Mo et al., 2021). In the troposphere, TMB is primarily oxidized via hydroxyl radical (OH), producing multigenerational oxidized compounds that can contribute to SOA formation and growth (Zaytsev et al., 2019; Mehra et al., 2020). The OH oxidation of TMB can also generate small dicarbonyls glyoxal and methylglyoxal (Zaytsev et al., 2019), which are significant precursors for light-absorbing SOA formation. Previous experimental studies have ascertained the importance of TMB-derived SOA (Liu et al., 2012; Zaytsev et al., 2019). However, the oxidation mechanism of TMB has not been updated in the Master Chemical Mechanism since 2005. To better understand TMB-SOA formation and growth, detailed laboratory characterization of TMB-SOA composition and TMB oxidation mechanisms with inorganic perturbation are required.

The mechanisms leading to secondary aerosol formation in the urban environment remain highly elusive and controversial, particularly for the processes related to changes in secondary aerosol mass and chemical composition. Recent studies have suggested that inorganic polluted emissions could perturb SOA formation, yet very little is known about the SO_2 and NH_3 effects on SOA formation. Given the ubiquity of SO_2, NH_3, and TMB, a key goal of this work is to determine the detailed formation mechanisms and chemical composition of secondary aerosol from TMB photooxidation with SO_2 and/or NH_3. We investigated the effects of SO_2 and NH_3 on the growth of particles from TMB photooxidation for the first time and discussed the role of inorganic species in TMB chemistry. The chemical composition of TMB SOA was rigorously characterized based on laboratory measurements. We revealed some hitherto unidentified organosulfates and tentatively proposed relevant formation pathway of products.

2 Experimental methods

2.1 Particle generation

Aerosol particles were produced from TMB photooxidation in the presence of NO_x in a new indoor smog chamber, which consists of a 1.1 m^3 Teflon reactor (0.6 mm Teflon film) housed in a temperature-controlled room. For photooxidation,

https://doi.org/10.5194/acp-2021-61
Preprint. Discussion started: 22 January 2021


Atmospheric Chemistry and Physics Discussions

a panel of black light lamps (F40BLB, GE) were used to provide ultraviolet (UV) irradiation centered at 365 nm. Before each run, the chamber was continually purged with dry and purified air prepared by zero air supply (Model 111, Thermo Scientific, USA) and simultaneously irradiated with UV lights until the concentrations of background contaminants (i.e., NO, NO_2, SO_2, and O_3) were lower than 1 ppb and the particle number concentration was below 5 cm^{-3}.

The TMB photooxidation experiments were carried out by the following steps. First, a known volume of TMB liquid (98%, Aladdin) was transported into the chamber through a heated (80 °C) Teflon tube carried by a flow of zero air. Second, according to experimental design, different quantities of NO (504 ppm in N_2, Qingdao Yuyan Gas Company, China), SO_2 (1013 ppm in N_2, Qingdao Yuyan Gas Company, China), and NH_3 (497 ppm in N_2, Qingdao Yuyan Gas Company, China) were introduced into the chamber from corresponding high-pressure cylinders using calibrated mass flow controllers (D07-7, Beijing Sevenstar Electronics Co., Ltd, China). Note that before the injection of NH_3, the inlet tubes were flushed with NH_3 flow for 30 min to minimize the adsorption losses of NH_3 in the tubes. After all species in the chamber were well mixed (initial concentrations of TMB, NO, and/or SO_2 were constant), black light lamps were turned on, marking the beginning of photooxidation experiments. The chamber was operated in batch mode with a reaction time of approximately 300–360 min. Temperature and relative humidity (RH) inside the chamber were (289 ± 4) K and (25 ± 1) %, respectively. Detailed experimental conditions and results for each experiment are provided in Table 1. Twelve experiments were conducted under four different scenarios. In the first set of experiments (Exps. 1–4, Table1), SO_2 levels in the chamber varied from 0 to 200 ppb while the initial ratio of [TMB] to [NO_x] was kept higher than 10 ppbC ppb^{-1} (low-NO_x condition). The second set of experiments (Exps. 5–8, Table1) were performed under high-NO_x condition ($[TMB]_0/[NO_x]_0$ < 10 ppbC ppb^{-1}) with SO_2 concentration being the only variable (ranged from 0 to 228 ppb). The third part of experiments (Exps. 9–10, Table1) consisted of an irradiation of TMB, NO_x, and NH_3, while the subsequent part of experiments (Exps. 11–12, Table1) consisted of an irradiation of TMB, NO_x, SO_2, and NH_3.

Different physicochemical parameters were measured over the course of photooxidation experiments. A digital thermo-hydrometer (Model 645, Testo AG, Lenzkirch, Germany) was used to measure temperature and RH inside the chamber. The concentrations of NO and NO_x were measured with a NO-NO_2-NO_x analyzer (model 42i, Thermo scientific, USA), while a Thermo scientific model 43i-TLE pulsed fluorescence SO_2 analyzer was used to measure SO_2 levels throughout the experiments. The O_3 level was monitored with a Thermo scientific model 49i O_3 analyzer. The initial concentration of NH_3 was calculated based on the introduced amount of NH_3 and the reactor volume. The decay of TMB was measured by a gas chromatography (GC, 7890B, Agilent Technologies, USA) equipped with a DB-624 column (30 m × 0.32 mm, 1.8 μm film thickness, Agilent Technologies, USA) and a flame ionization detector (FID). The GC temperature was

https://doi.org/10.5194/acp-2021-61
Preprint. Discussion started: 22 January 2021

Atmospheric Chemistry and Physics Discussions

programmed to increase from 80 to 200 °C at 20 °C min^{-1} rate. Particle size distributions and volume concentrations in all experiments were recorded in situ using a scanning mobility particle sizer (SMPS), which consists of a long differential mobility analyzer (long-DMA, Model 3082, TSI, USA) and a condensation particle counter (CPC, Model 3776, TSI, USA). The long-DMA was available for measuring the particle size distribution in the range of 13.8–723.4 nm while smaller particles between 4.5–162.5 nm were measured with a nano differential mobility analyzer (nano-DMA, Model 3085, TSI, USA). The measured volume concentration in each experiment was converted into particle mass concentration with an estimated particle density of 1.4 g cm^{-3}.

Table 1. Experimental conditions and results for the TMB photooxidation experiments.

Exp.	$[TMB]_0$ (ppb)	$[TMB]_0/[NO_x]_0$ (ppbC ppb^{-1})	$[NO_x]_0$ (ppb)	$[SO_2]_0$ (ppb)	$[NH_3]_0$ (ppb)	$[OH] \times 10^{-6}$ (molecules cm^{-3}) [a]	$N_{max} \times 10^{-5}$ (cm^{-3}) [b]	SOA ($\mu g\ m^{-3}$) [c]	SOA yield (%) [d]
1	374	18.9	178	-	-	2.52	0.27	52.6	3.8 ± 0.4
2	350	17.3	182	59	-	2.33	1.12	97.8	8.2 ± 0.7
3	368	17.3	191	107	-	2.29	1.13	164.8	12.6 ± 1.3
4	220	10.0	199	200	-	3.00	1.40	175.6	17.6 ± 2.0
5	393	7.6	465	-	-	3.62	0.29	59.4	3.5 ± 0.4
6	346	6.8	457	68	-	3.44	0.93	120.7	7.9 ± 0.7
7	260	5.1	457	114	-	3.12	0.98	78.7	8.0 ± 0.7
8	379	7.4	464	228	-	3.06	1.10	186.9	12.2 ± 1.2
9	454	8.6	475	-	100	3.42	0.45	70.6	3.8 ± 0.4
10	464	9.1	457	-	200	3.37	0.60	99.3	5.1 ± 0.5
11	425	8.6	447	227	100	3.51	1.57	209.6	12.9 ± 1.3
12	450	8.9	455	234	200	3.32	2.00	244.9	13.7 ± 1.4

[a] The average OH concentration was determined from the measured TMB decay. [b] Aerosol particles maximum number concentration. [c] SOA mass concentrations have been wall-loss corrected. [d] Uncertainties in SOA yield were calculated from uncertainties propagation using the sum of the uncertainties in TMB data and the systematic error of SMPS.

https://doi.org/10.5194/acp-2021-61
Preprint. Discussion started: 22 January 2021


Atmospheric Chemistry and Physics Discussions

2.2 Particle collection and analysis

2.2.1 Attenuated total reflectance-Fourier transform infrared spectroscopy analysis

Following 300–360 min of reaction, aerosol samples were collected onto aluminum foils (25 mm, Jowin Technology Co. Ltd.) by a low-pressure impactor (DLPI+, DeKati Ltd, Finland) and were stored at -20 ℃ thereafter until analysis to reduce evaporative losses of aerosol. The chemical functional groups of aerosols were characterized by an attenuated total reflectance-Fourier transform infrared (ATR-FTIR) spectrophotometer (Vertex 70, Bruker, Germany) with mercury cadmium telluride detector. The ATR-FTIR spectra of aerosol particles in each run were recorded by averaging 64 scans from 4000–600 cm^{-1} with a resolution of 4 cm^{-1}. Prior to each measurement with ATR-FTIR, the surface of the diamond crystal was thoroughly cleaned with ethanol and ultrapure water to rule out interferences of other sources of contamination. The ATR-FTIR spectra of blank aluminum foils were also acquired to confirm the absence of IR absorption by the aluminum foil on which aerosols are collected.

2.2.2 Ion chromatography analysis

Following the ATR-FTIR measurements, aerosol samples were extracted in 3 mL of ultrapure water (Milli-Q water, 18.2 MΩ) under sonication in an ice bath for 30 min. The extracted samples were filtered through polyethersulfone syringe filters (0.22 μm pore size) and subsequently analyzed for their ionic concentrations using an ion chromatography (Dionex ICS-600, Thermo Fisher Scientific, USA) with electrical conductivity detection. A Dionex IonPac™ AS19 column (4 × 250 mm) connected with AG19 guard column (4 × 50 mm, Dionex Ionpac) was used to separate anions. An aqueous solution of 20 mM potassium hydroxide (KOH) prepared by reagent-free controller (Dionex, Thermo Scientific, USA) was used as anion eluent. Cation analysis was carried out with the pair of CG12A guard column (4 × 50 mm, Dionex Ionpac) and analytical column (4 × 250 mm, CS12A, Dionex IonPac™) and an isocratic 20 mM methanesulfonic acid (CH_4O_3S). The same volume of extract was injected into the ion chromatograph by a six-way valve mounted with a loop of 250 μL. The elution flow rates of KOH and CH_4O_3S were both set to 1 L min^{-1}.

2.2.3 Ultra-high-performance liquid chromatography high resolution mass spectrometry analysis

Laboratory-generated aerosols were also collected on 47 mm polytetrafluoroethylene (PTFE) filters (0.22 μm pore size, Tianjin Jinteng Experimental Equipment, China) using a stainless steel inline filter holder (Sartorius 16254, Sartorius

https://doi.org/10.5194/acp-2021-61
Preprint. Discussion started: 22 January 2021


Atmospheric Chemistry and Physics Discussions

Stedim Biotech GmbH, Germany) with a flow rate of 10 L min^{-1}. The collected samples were wrapped in foil and stored in the freezer (-20 ℃) until mass spectrometry analysis. Filter samples were extracted twice with 5 mL of high-purity methanol (Optima® LC-MS grade, Fisher Scientific) under sonication in ice for 30 min. The extracts were mixed, filtered with a 0.2 μm pore size PTFE syringe filter (Millipore), and concentrated to near dryness under a gentle stream of high-purity nitrogen. The concentrated samples were reconstituted with ultrapure water (Milli-Q water, 18.2 MΩ) and methanol (Optima® LC-MS grade, Fisher Scientific) with a volume ratio of 50:50. A control mass spectrometry measurement of solvent and extracts from blank PTFE filters were preformed to remove the interferences of solvent and handling protocols. The chemical compositions of aerosols were characterized using an ultra-high-performance liquid chromatography (UPLC, Ultimate 3000, Thermo scientific, USA) coupled to a Q-Exactive Focus Hybrid Quadrupole-Orbitrap mass spectrometry (MS, Thermo Scientific, USA) with electrospray ionization (ESI). The ESI source was operated in both positive (+) and negative (-) ionization mode. Product molecules could be detected as $[M + H]^+$ in the positive ion mode while products could be ionized via deprotonation and were detected as $[M - H]^-$ in the negative ion mode. The following parameters were set for the optimal operation of LC/ESI-MS: spray voltage (+), 3.5 kV; spray voltage (-), -3.0 kV; S-lens RF level (+), 50 V; S-lens RF level (-), 50 V; capillary temperature, 320 °C; sheath gas (nitrogen) pressure, 2.76×10^5 Pa; auxiliary gas (nitrogen) flow, 3.33 L min^{-1}. MS spectra were recorded in the range of m/z 50 to 750 in full MS scan, which was followed by data-dependent scans (DDA) using stepped collision energies of 20, 40, and 60 eV via high-energy collisional dissociation to obtain MS/MS data. The separation of analytes was carried out on an Atlantis T3 C18 column (100 Å, 3 mm particle size, 2.1 mm × 150 mm, Waters, USA) at 35 ℃. The mobile phases consisted of (A) 0.1% formic acid (Optima® LC-MS grade, Fisher Scientific) in ultra-pure water (Milli-Q water, 18.2 MΩ) and (B) 0.1% formic acid in methanol (Optima® LC-MS grade, Fisher Scientific). The injected volume of samples was 2 μL in this study. Samplers were eluted using a 60-min gradient elution program with a flow rate of 200 μL min^{-1}: initially set to 3% over the first 3 min, the concentration of eluent B was increased linearly to 50% in 22 min, from 50% to 90% from 25 min to 43 min, then it was decreased from 90% to 3% from 43 to 48 min, and finally kept at 3% for 12 min. The chemical formulas of observed ions were proposed based on reaction pathways, chemical consideration, and measured m/z value with a mass tolerance of ± 5 ppm. All data were recorded and processed using Xcalibur V4.2.47 software package.

2.3 Wall losses of vapors and particles

The SOA yield, usually used to quantify the propensity of a parent hydrocarbon to form SOA, could be determined as

https://doi.org/10.5194/acp-2021-61
Preprint. Discussion started: 22 January 2021


Atmospheric Chemistry and Physics Discussions

the ratio of the generated particle mass to the amount of consumed parent hydrocarbon. The particle and vapor wall depositions in chambers can lead to the underestimation of the SOA yield. In order to determine the particles wall loss rates, ammonium sulfate particles were introduced into the chamber using a constant output atomizer (Model 3706, TSI, USA) with an aqueous solution of ammonium sulfate. The size-dependent loss rate (k_{dep}) of ammonium sulfate particles could be expressed as $k_{dep} = 5.5\times10^{-6}\times D_p^{1.05} + 0.18\times D_p^{-1.19}$ and was applied to correct the aerosol particle concentrations. The wall loss rates of NO, NO_2, SO_2, and TMB were determined to be 2.0×10^{-6}, 3.9×10^{-6}, 4.0×10^{-7}, and 2.3×10^{-6} s^{-1}, respectively, indicating that the wall losses of these species were negligible over the course of the experiment. However, gas-phase species that could deposit to the chamber walls include not just the parent hydrocarbon, in this case TMB, but also the oxidation products, which in general are not all totally monitored and characterized. It is difficult to correct directly and accurately for the impact of vapor wall losses on the measured SOA yield. Therefore, the observed SOA yield in this work is only the lower limit. Here, the underestimation of SOA yields due to vapor wall losses was roughly determined by the method in the study of Zhang et al. (2014). In brief, the effect of vapor wall losses on SOA yield in the chamber significantly arose from the competition between vapors condensation onto aerosol particles versus vapor depositions to chamber walls. The extent to which vapor wall depositions influence the SOA yield could be estimated by the ratio of the average timescale of gas-particle partitioning during the photooxidation experiments to the timescale of vapor wall deposition. The evaluated results suggested that the SOA yield could be underestimated by a factor of 1.8 to 8.4 without accounting for vapor losses.

3 Results and discussion

3.1 Effects of SO_2

3.1.1 Particle formation and growth in SO_2-added photooxidation

To evaluate the impacts of SO_2 on aerosol formation and growth from TMB photooxidation, a series of experiments were conducted with various initial SO_2 levels under both low- and high-NO_x conditions. Evolutions of the number distributions of secondary aerosols with particle size within 4.5–162.5 nm are provided in Fig. 1. There was no new secondary aerosol formation in the beginning of photooxidation. After a period of time, particles were burst produced and the number concentration of particle increased rapidly. At the same time, the particles continuously grew via condensation and then coagulation mechanisms, consistent with a previous study (Jorga et al., 2020). After 300 min UV irradiation without SO_2 introduction, the total maximum number concentration of aerosol particles was only 2.7×10^4

https://doi.org/10.5194/acp-2021-61
Preprint. Discussion started: 22 January 2021

Atmospheric Chemistry and Physics Discussions

240 cm^{-3} and 2.9×10^4 cm^{-3} under low- and high-NO_x conditions, respectively (Table 1). Interestingly, the particle formation is considerably promoted in the presence of SO_2. With the introduction of 200 ppb SO_2 in low-NO_x, the maximum particle number concentration was as high as 1.4×10^5 cm^{-3}, which is 4.2 times higher than that in TMB/NO_x photooxidation. In high-NO_x systems, the maximum particle number concentration increased by 2.8 times in the presence of 228 ppb SO_2. It should be noted that particles with mobility diameter ranging from 10 to 80 nm, especially, dominated 245 particle number concentrations with SO_2 addition (Fig. 1). Ultrafine particles with diameter below 100 nm are more harmful to human than larger particles because they can more easily penetrate deep into the lungs and blood circulation (Terzano et al., 2010). Our results indicate that SO_2 concentration is a key parameter for ultrafine particle formation. It has been suggested that reducing the number concentration of ultrafine particles can decrease mortality, highlighting again the need to continue to implement strict SO_2 emissions standards (Fuzzi et al., 2015).

250

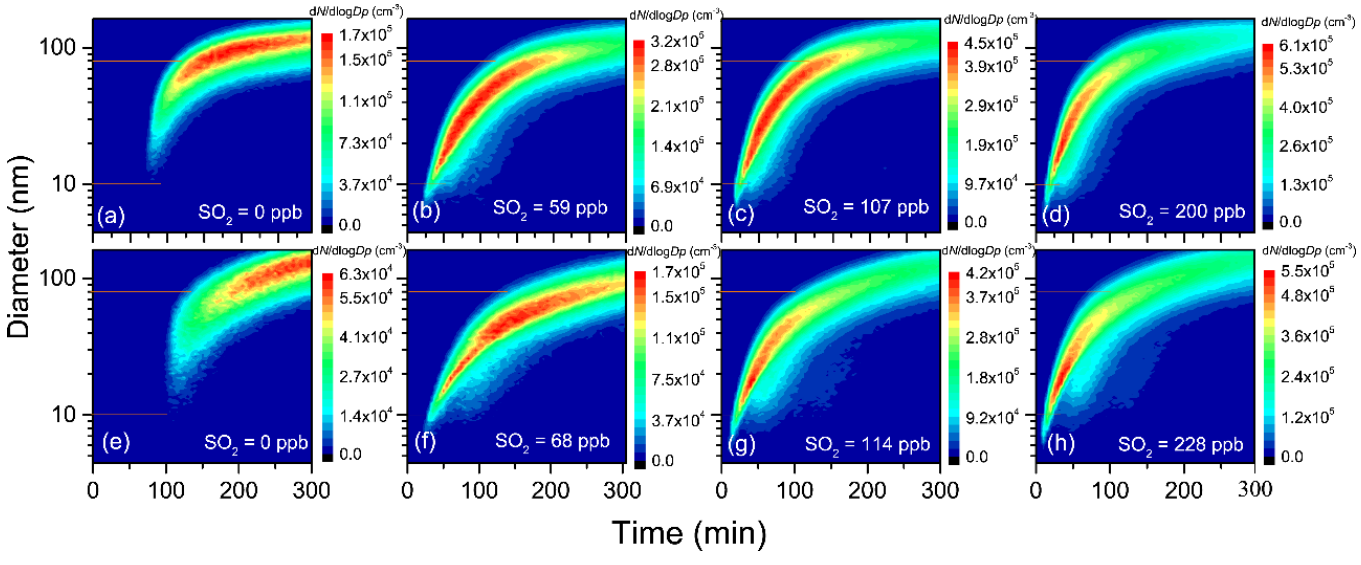

Figure 1. Evolutions of the number distributions of aerosol particles generated from TMB photooxidation in low-NO_x (Panels a–d) and high-NO_x experiments (Panels e–h).

255 To fully give account for effects of changes in SO_2 emissions on aerosol formation, the key particle phase parameters (i.e., nucleation time, initial growth rate, and mean particle diameter) as a function of SO_2 levels are further compared in Fig. 2. In the present study, the SMPS instrument can measure particle larger than 4.5 nm and, therefore, the nucleation time here is defined as the time required for new secondary aerosols to grow to 4.5 nm after the lights have been turned

https://doi.org/10.5194/acp-2021-61
Preprint. Discussion started: 22 January 2021


Atmospheric Chemistry and Physics Discussions

on (Wyche et al., 2009).The particle size rapidly increased within 30 min after nucleation, and gradually reached a stable level (Fig. 1). Consequently, the initial growth rate (GR_{inital}), calculated based on the method of Kulmala et al. (2012), is defined as the particle growth rate within 30 min after nucleation (Li et al., 2018). From Fig. 2, a significant negative correlation was found between nucleation time and initial SO_2 level. Furthermore, when similar amounts of SO_2 were introduced to the reaction mixture, the gap between the nucleation time of low-NO_x and high-NO_x would be reduced, which is in agreement with a previous study (Zhao et al., 2018). Under SO_2-free condition, new secondary aerosol could be generated by homogeneous nucleation involving key intermediate products of TMB oxidation. The delay time for particle formation largely corresponds to the time required for intermediate products to build to sufficient concentrations in such a way that their saturation vapor pressure relative to the particle phase is exceeded. New secondary aerosol consists of later stage oxidation products, which might be also responsible for the delayed occurrence. It was demonstrated that higher OH concentration in the chamber could result in faster particle formation (Sarrafzadeh et al., 2016). However, the average OH concentration in SO_2-free experiments is comparable with that in SO_2-added experiments (Table 1). There has been a gradual fall in the mixing ratio of SO_2 that could be oxidized to sulfuric acid (H_2SO_4) during TMB photooxidation (Fig. S1). H_2SO_4 is a critical compound involved in new particle formation, which could provide condensed surface for key compounds. Therefore, the small nucleation time in TMB/NO_x/SO_2 photooxidation is largely attributed to H_2SO_4 formation. The mean diameter of secondary aerosol decreased by 4–10 nm when 60–70 ppb of SO_2 was included in the matrix (Fig. 2). In contrast, at high-SO_2 levels ($[SO_2]_0 > 100$ ppb), increase in the initial SO_2 concentration led to an increase in particle mean diameter, regardless of low- or high-NO_x. The initial growth rate also showed a similar dependence on the SO_2 level as presented in Fig. 2. The nonlinear response of the mean particle diameter to SO_2 initial concentration might be due to the nonlinear dynamics of aerosol particle populations (Julin et al., 2018). Particle size can influence water vapor uptake by particles and thus might impact the lifetime of particles in the atmosphere (Fuzzi et al., 2015).

https://doi.org/10.5194/acp-2021-61
Preprint. Discussion started: 22 January 2021

Atmospheric Chemistry and Physics Discussions

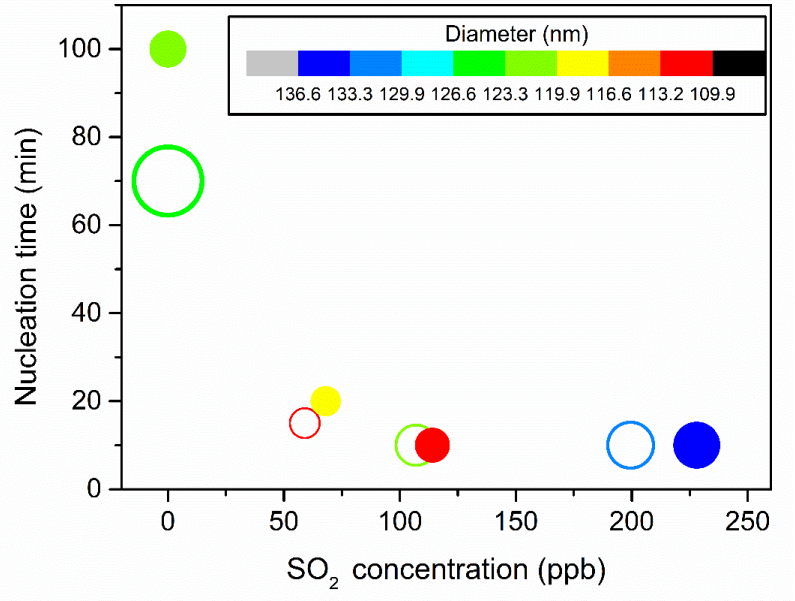

Figure 2. Nucleation time of particle as a function of initial SO_2 concentration for low-NO_x (open circles) and high-NO_x (solid circles) conditions (Exps. 1–8). Symbol color indicates the mean diameter of particle and symbol size the initial growth rate of particle.

3.1.2 SOA yield in SO_2-added photooxidation

The particle volume concentration as a function of TMB consumption is presented in Fig. 3, where it can be observed that the particle formation increased with increasing initial SO_2 levels regardless of low- or high-NO_x conditions. The present result is consistent with a previous research, which found that limonene SOA formation is significantly promoted with SO_2 addition (Ye et al., 2018). SO_2 was found to perturb particle formation by inducing chemical reactions in both the gas- and particle-phase (Wang et al., 2019a; Friedman et al., 2016). We are unable to fully rule out the SO_2 impacts on gas-phase chemistry. However, the decay of TMB was essentially unchanged when SO_2 was introduced into the chamber (Fig. S2), which suggests the unlikeliness of SO_2 addition to affect the gas-phase chemistry of TMB photooxidation (Kleindienst et al., 2006). Instead, it is more likely attributed to the formation and condensation of H_2SO_4 and/or the enhancement of organic aerosols formation. As presented in Fig. S3, the inorganic sulfate concentration, from H_2SO_4 generated in the chamber, has a positive relationship with initial SO_2 level. Sulfate and nitrate were found to account for a large portion of the inorganic component based on IC measurements of generated particle. In order to

https://doi.org/10.5194/acp-2021-61
Preprint. Discussion started: 22 January 2021

Atmospheric Chemistry and Physics Discussions

calculate the SOA yield, the inorganic mass concentration was subtracted from the particle mass concentration. The influence of SO_2 initial level on SOA yield can be seen in Table 1 as high SO_2 levels contribute to produce somewhat high SOA yields. Figure 4 compares the SOA yields obtained from the present work with those found in previous studies with similar experimental conditions. SOA yields from the two SO_2-free experiments are comparable to that reported from the study of Liu et al. (2012) and fit quite well with the yield curve of Odum et al. (1996). The SOA yields in our TMB/NO_x photooxidation experiments were 3.8% and 3.5%, which were closed to 3.9% and 4.2% derived from yield curve of Odum et al. (1996) under same mass concentration. In contrast, with similar mass concentration, the SOA yields in SO_2-added regimes were higher than those in previous studies (Odum et al., 1996; Liu et al., 2012). Here the neutralization degree of particle, which was calculated as the molar ratio of NH_4^+ to the sum of SO_4^{2-} and NO_3^- (Lin et al., 2013), was used as a tool to roughly estimate the aerosol acidity of collected particle samples. The value of neutralization degree were lower than 1 in this work, indicating acidic aerosols (Lin et al., 2013). The increase in aerosol acidity could be largely responsible for the observed enhancements in SOA formation in SO_2-invloved experiments. The OH oxidation of TMB can result in the formation of multifunctional carbonyl compounds (Liu et al., 2012; Zaytsev et al., 2019), which could promote SOA formation via acid-catalyzed heterogeneous reactions.

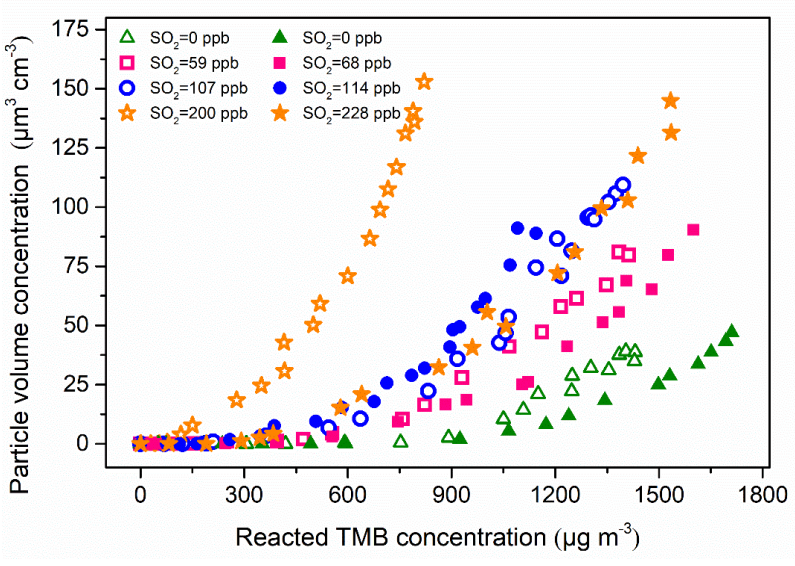

Figure 3. Growth of particle volume concentrations from TMB photooxidation as a function of TMB consumption for eight experiments with different initial SO_2 concentrations (Exps. 1–8). The open symbols and solid symbols represent low- and high-NO_x experiments, respectively.

https://doi.org/10.5194/acp-2021-61
Preprint. Discussion started: 22 January 2021

Atmospheric Chemistry and Physics Discussions

315

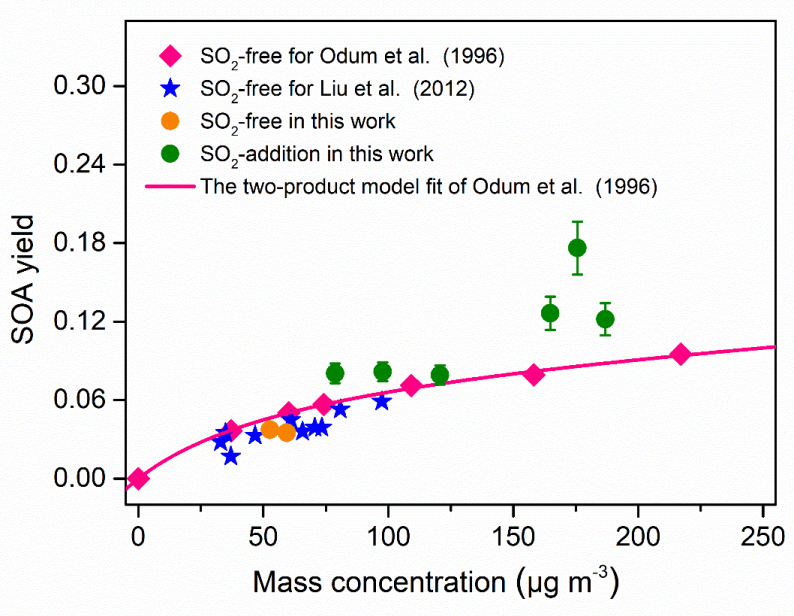

Figure 4. Comparison of SOA yields from TMB photooxidation as a function of SOA mass concentration with data reported from literature. The SOA density in the whole study was assumed to be 1.4 g cm^{-3}. The SOA yields for Liu et al. (2012) were extracted from Table 1 in the study. The pink line is the best fit two-product model for the SOA yields and was extracted from Figure 2 in the work of Odum et al. (1996).

3.1.3 Particle chemical composition in SO_2-added photooxidation

Aerosol particles contain a multitude of compounds with different physiochemical properties, having various impacts on climate and human health. In order to investigate the effects of SO_2 on the chemical composition of aerosol particles, the particles were first characterized by ATR-FTIR. Figure 5 compares the characteristic ATR-FTIR spectra of particles formed from the photooxidation of TMB under different conditions and the detailed information on the assignment of absorption peaks are given in Table S1. For the samples collected from SO_2-free photooxidation, the particles exhibited an O-H stretch at 3600–3000 cm^{-1} as shown in Fig. 5(a) and (b). The C=O stretch of carbonyl at 1720 cm^{-1} suggests that aldehydes, ketones, and carboxylic acids are significant particle components, while the absorptions at 844 cm^{-1} (NO symmetric stretch), 1284 cm^{-1} (NO_2 symmetric stretch), and 1647 cm^{-1} (NO_2 asymmetric stretch) are the characteristic peaks of organic nitrates. The slight absorbance at 941 cm^{-1} indicates the presence of peroxides containing O-O groups.

https://doi.org/10.5194/acp-2021-61
Preprint. Discussion started: 22 January 2021

Atmospheric Chemistry and Physics Discussions

Interestingly, compared with the particles from SO_2-free experiments, there was a new peak at 615 cm^{-1} for the particles generated from SO_2-added experiments, regardless of low- or high-NO_x conditions. The 615 cm^{-1} peak is characteristic of inorganic sulfates, and further highlights that the presence of SO_2 promotes the formation of inorganic sulfates as pointed out in previous studies (Chen et al., 2019; Liu et al., 2016). The strong absorption at 1081 cm^{-1} arises from the S=O bands in the particle components. Field and laboratory studies have reported that inorganic sulfate could convert into organosulfur compounds in the atmosphere (Riva et al., 2019; Nestorowicz et al., 2018). Therefore, the peak at 1081 cm^{-1} may be mainly from the absorption of both inorganic sulfates and organosulfur compounds.

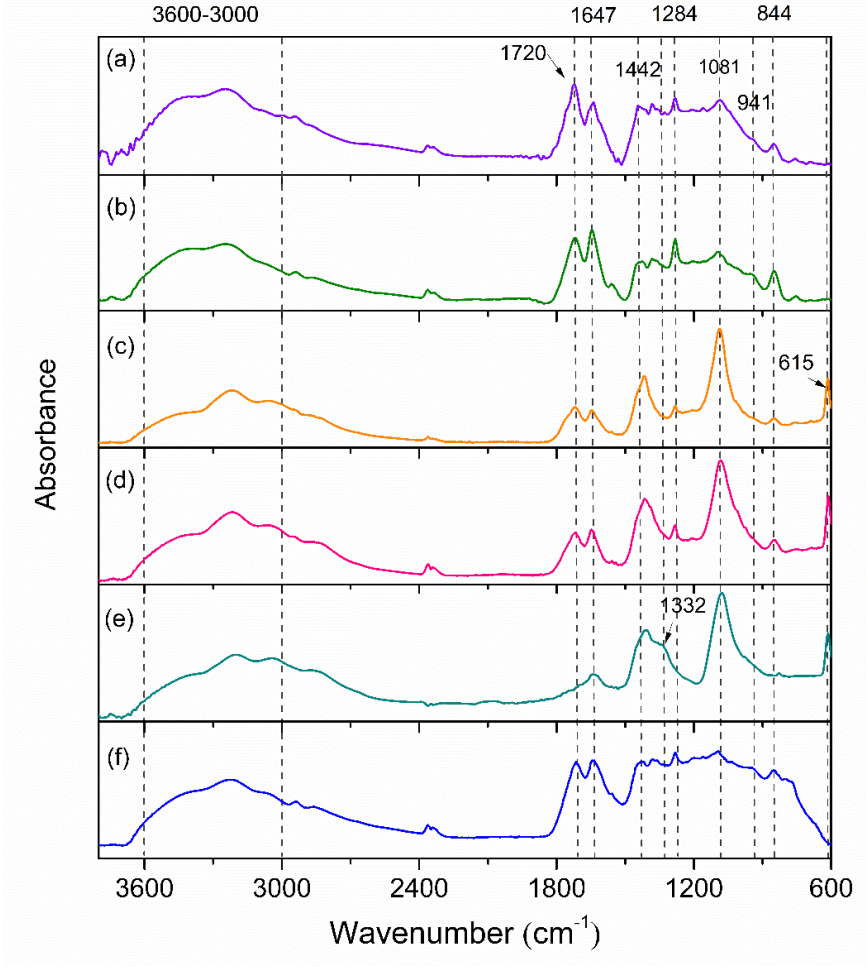

Figure 5. ATR-FTIR spectra of aerosol particles generated from (a–b) TMB/NO_x, (c–d) TMB/NO_x/SO_2, (e) TMB/NO_x/NH_3/SO_2, and (f) TMB/NO_x/NH_3 photooxidation.

https://doi.org/10.5194/acp-2021-61
Preprint. Discussion started: 22 January 2021


Atmospheric Chemistry and Physics Discussions

The chemical compositions of particles generated in TMB/NO_x and TMB/NO_x/SO_2 photooxidations were further measured with high-resolution mass spectrometry (HRMS), to determine whether organosulfur compounds were formed in SO_2-added experiments. The formation of organosulfur compounds was recognized by the oxidation mechanism and the loss of characteristic fragment ions at m/z 79.95 (SO_3^-), 80.96 (HSO_3^-), and 96.96 (HSO_4^-) in MS/MS spectra (Figs. S4-S5). The list of compounds observed in this work along with molecular weights (MW), measured masses and proposed structures are presented in Table S2. In SO_2-free experiments, the major aerosol components were multifunctional alcohols, peroxides, organic nitrates, ketoaldehydes, and ketocarboxylic acids. With the same analytical methods, the same products were also observed in SO_2-added photooxidation. The most striking result to emerge from Table S2 is that ten organosulfates (OS-214, OS-226, OS-228, OS-240, OS-242, OS-244, OS-268, OS-300, OS-316, and OS-345) and two organic sulfonates were only detected in filter samples collected from the TMB/NO_x/SO_2 photooxidation experiment, indicating that SO_2 emissions in the atmosphere can alter the aerosol formation chemistry and thus influence the aerosol chemical composition. To the best of our knowledge, this is the first time the ten organosulfates are identified in TMB/NO_x/SO_2 photooxidation experiments. Recently, some sulfur-containing compounds from field measurements were designated as compounds of unknown origin. For example, the MW 214 organosulfate has been detected in $PM_{2.5}$ collected from the highly polluted megacity Shanghai (Cai et al., 2020). However, the VOC precursor for this organosulfate formation was not reported. The MW 242 organosulfate found in Baengnyeong Island was also classified as organosulfur of unknown origin (Boris et al., 2016). O'Brien et al. (2014) found the formation of MW 228 organosulfate in ambient aerosol particles but its specific source was not pointed out. Evidence from this study suggests that TMB photooxidation in the presence of SO_2 might contribute to the formation of these organosulfates (MW = 214, 228, and 242) in the ambient air. Importantly, an organosulfur compound with a formula of $C_7H_{12}O_7S$ (MW = 240) was observed in ambient fine aerosols and was assigned to an oxidation product of anthropogenic 1,3,5-trimethylbenzene (Boris et al., 2016). The finding of the current study suggests that the organosulfur compound (MW = 240) may also be produced from the photooxidation of 1,2,4-trimethylbenzene in the presence of SO_2. In addition, in the absence of authentic standard and chromatographic conditions, the MW 226, 240, and 268 organosulfur compounds were designated as biogenic-derived organosulfates in previous field studies (Cai et al., 2020; Boris et al., 2016). Our results show the detection of OS-226, OS-240, and OS-268 organosulfates, which are also isomers of organosulfates derived from isoprene (Cai et al., 2020), limonene (Cai et al., 2020), and limonene (Boris et al., 2016), respectively. More studies need to be undertaken to differentiate various sources of organosulfates in the ambient aerosols through chemical synthesis of authentic organosulfates standards.

https://doi.org/10.5194/acp-2021-61
Preprint. Discussion started: 22 January 2021


Atmospheric Chemistry and Physics Discussions

370

The mechanisms describing the formation of OS-226, OS-228, OS-240, OS-242, OS-244, OS-300, OS-316, and OS-345 are proposed in Fig. 6. Following analogous mechanisms for toluene photooxidation, the oxidation of TMB is dominantly initiated by OH addition to the benzene ring to form TMB-OH adduct, which can react with O_2 through recombination
375 to produce bicyclic peroxy radical. It has been established that a series of ring-retaining (product A in Fig. 6) and ring-opening products (products B, C, and D in Fig. 6) can be generated by the further reaction of bicyclic peroxy radical in the presence of NO (Zaytsev et al., 2019; Li and Wang, 2014). Both ring-opening and ring-retaining compounds are expected to contribute significantly to organosulfate production. Here, we take unsaturated ketoaldehyde (product C in Fig. 6) as an example to describe the possible formation mechanism of organosulfate observed in the present study. The
380 reaction of OH with compound C involves OH addition to unsaturated C=C bonds to form an alkyl radical, which can react subsequently with O_2 to yield organic peroxy radical. Further reactions of organic peroxy radical can follow two different pathways. One pathway is that the organic peroxy radical undergoes a 1,5-H-shift isomerization to form a new acyl radical. Insight from a previous review suggested that acyl radical react with O_2 to yield acylperoxy radical, which could further react with HO_2 to form multifunctional hydroperoxide (Ziemann and Atkinson, 2012). The second channel
385 is the reaction of organic peroxy radical with HO_2 to produce hydroperoxide, terminating directly the radical chain. Acid-driven heterogeneous chemistry of hydroperoxide has been previously adopted to explain the generation of certain OSs (Riva et al., 2016a; Riva et al., 2016b). With the presence of sulfuric acid formed by the oxidation of SO_2 by OH, TMB-derived hydroperoxides can be hydrolyzed by H^+ and then react with inorganic SO_4^{2-} to form organosulfate. Recently, the significance of inorganic sulfates conversion to organosulfates was demonstrated by Riva et al. (2019), who suggested
390 that the considerable conversion of inorganic sulfates to organosulfates can cause the changes in aerosol growth, multiphase chemistry, acidity, and cloud condensation nuclei activity.

https://doi.org/10.5194/acp-2021-61
Preprint. Discussion started: 22 January 2021

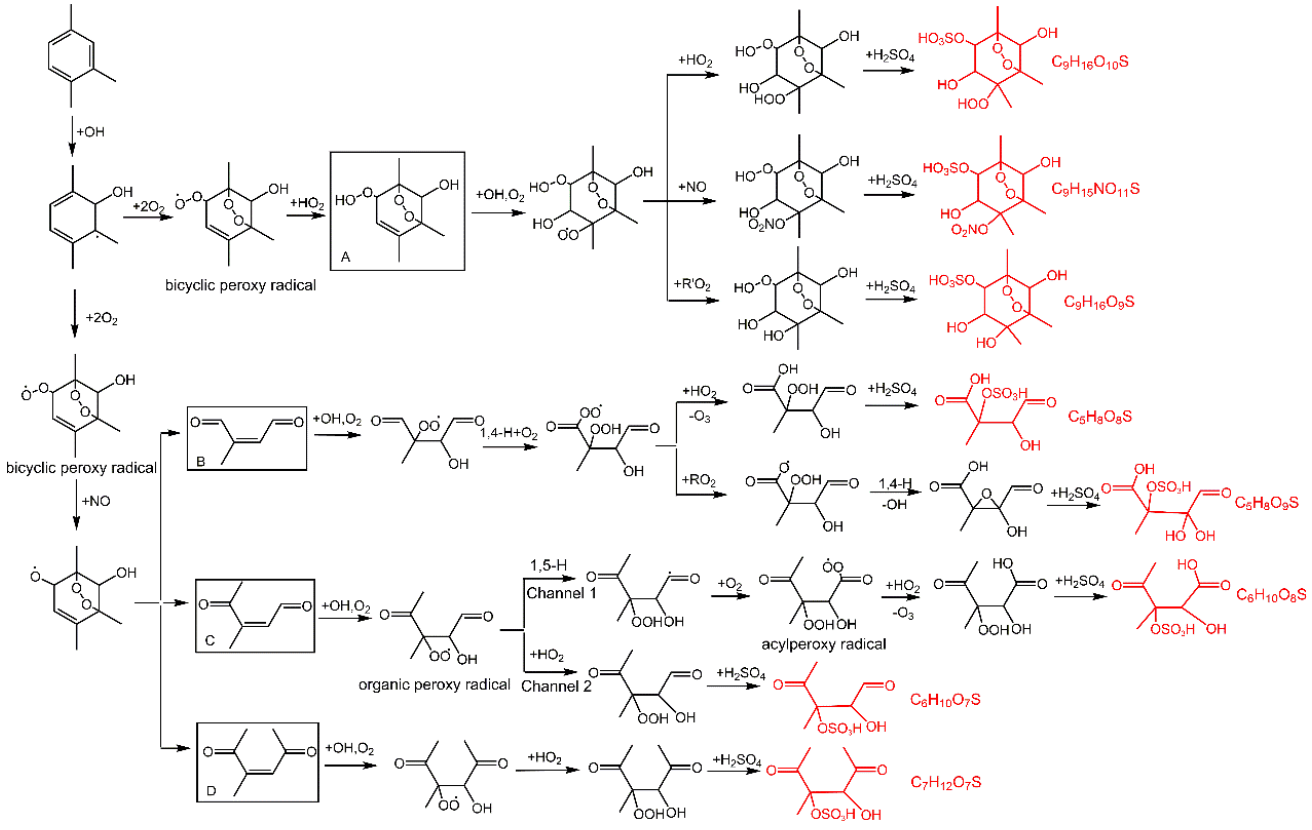

Figure 6. Proposed mechanisms for organosulfate formation from the photooxidation of TMB in the presence of SO_2. The black boxes mark the ring-opening and ring-retaining products suggested in previous studies (Li and Wang, 2014; Zaytsev et al., 2019). The compounds in red are organosulfates detected by UPLC-HRMS in this work.

The MW 228 and 230 organic sulfonates were assigned as sulfonates containing an aromatic ring based on accurate mass measurements and comparison of mass fragmentation patterns with other aromatic sulfonates (Riva et al., 2015a). MS/MS spectra and the proposed fragmentation schemes of sulfonates are reported in Fig. S5. For MW 228 sulfonate, the MS/MS spectra showed the fragment ions at m/z 79.95721 ($SO_3^{\cdot/-}$), 118.96625 ($C_8H_7O^-$, M - $SO_3^{\cdot/-}$ - CO), and 163.04025 ($C_9H_7O_3^-$, M - SO_2) as presented in Fig. S5. For the MW 230 sulfonate, the fragment of parent ion at m/z 229.01706 could occur by the loss of 44 mass units to give the product ion at m/z 185.02777 (Fig. S5). The loss of 79.95747 mass units as sulfite radical is in accord with the MS/MS spectra of aromatic sulfonates generated from the photooxidation of polycyclic aromatic hydrocarbons (Riva et al., 2015b). A recent field measurement demonstrated that

https://doi.org/10.5194/acp-2021-61
Preprint. Discussion started: 22 January 2021


Atmospheric Chemistry and Physics Discussions

aromatic organosulfur compounds account for a substantial fraction of total organosulfur compounds in Shanghai, highlighting the importance of aromatic organosulfur compounds (Ma et al., 2014). Aromatic sulfonates formation from the photooxidation of TMB in the presence of SO_2 was unexpected and the exact formation pathway of the aromatic sulfonates warrants further investigation.

3.2 Effects of NH_3

3.2.1 Particle formation and growth in NH_3-involved photooxidation

High-NO_x photooxidation experiments were carried out in the presence/absence of NH_3. The average OH concentrations were similar for each experiment within 300 min of irradiation (Table 1). Figure 7 displays the volume and number concentrations of aerosols as a function of time in different photooxidations (Exps. 5, 8–12). TMB was oxidized to produce many secondary aerosols under continuous UV irradiation. The volume concentrations of aerosol particles have a clear positive correlation with NH_3 initial level for all conditions, which might be ascribed to the formation of ammonium salts (Flores et al., 2014; Hao et al., 2020; Lu and Zhang, 2020). From Fig. 7, the influence of NH_3 on particle formation was not as pronounced as that of SO_2 with similar concentrations. However, measurements demonstrated that the coexistence of SO_2 and NH_3 can considerably promote aerosol particles formation. The result is in line with a previous study which showed that the synergetic effects of NH_3 and SO_2 could substantially increase the yield of SOA from the photooxidation of toluene (Chu et al., 2016). The total number concentrations of aerosol particles increased rapidly in all experiments after nucleation was initiated as shown in Fig. 7 (b). After reaching the maximum concentration, the number density of particles declined gradually because of particles coagulation and deposition to the chamber walls. An enhancement effect of NH_3 on the number concentrations of particles was also observed. Under SO_2-free condition, as the initial NH_3 concentration increased from 0 to 200 ppb, the maximum particle number concentration increased accordingly from 2.9×10^4 to 6.0×10^4 cm^{-3}. Under SO_2-involved conditions, increasing the NH_3 level to 200 ppb enhanced the particle maximum number concentration by a factor of 1.7. This demonstrates that the ability of particles formation originating from gas-to-particle conversion is significantly stronger with NH_3 introduction. Our results are valuable in terms of the potential of NH_3 emission reductions to improve air quality by decreasing total particle number concentrations.

https://doi.org/10.5194/acp-2021-61
Preprint. Discussion started: 22 January 2021

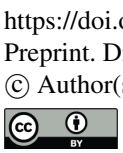

Atmospheric Chemistry and Physics Discussions

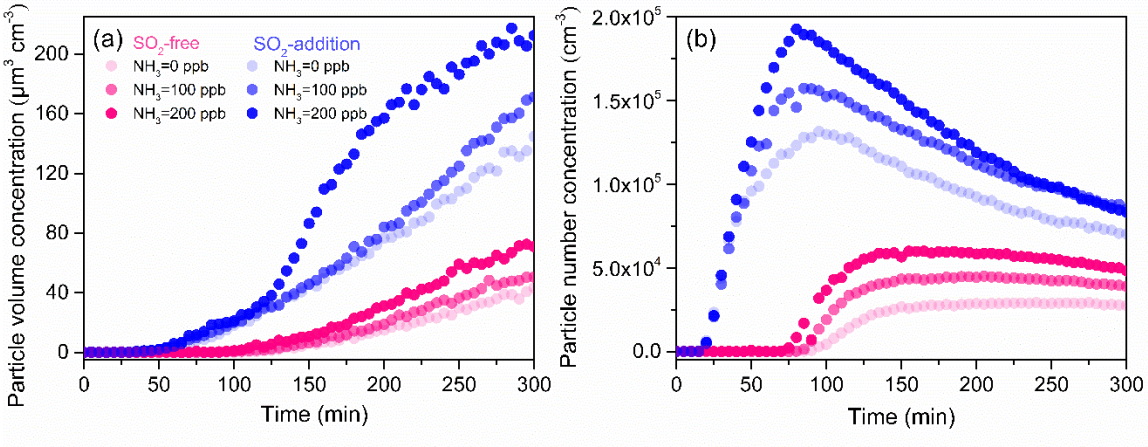

Figure 7. Time evolutions of the volume (a) and number (b) concentrations of aerosol particles from TMB photooxidation with different initial NH_3 levels under SO_2-free and SO_2-addtion (~ 230 ppb) conditions.

Once generated, aerosol particles need to grow to a larger size (> 50–100 nm) before they exert significant impact on global climate and public health. To explore the effects of NH_3 on particle growth, the initial growth rate of aerosol particles from different experiments are also compared in Fig. S6. Initial growth rate responded differently to reaction conditions as shown in Fig. S6. In SO_2-free experiments, the increase in NH_3 initial concentrations led to remarkable increase of the initial growth rate of aerosol particles. High initial growth rates were also found in the photooxidation of other aromatics such as toluene and o/m/p-xylene with NH_3 addition (Li et al., 2018). This result may be explained by the fact that under SO_2-free condition, NH_3 mainly reacts with nitric acid to produce ammonium salts. Previous studies have reported that ammonium salts could partition into the initial growth process of new secondary aerosol particles and thus increase the particle initial growth rate (Li et al., 2018; Zhu et al., 2014). More interestingly, NH_3 level did not substantially affect the initial growth rate of particles in the presence of SO_2 (Fig. S6). The results in Fig. 7 have demonstrated that the synergetic effects of NH_3 and SO_2 can promote new particle formation (Lehtipalo et al., 2018). In SO_2-involved experiments, NH_3 molecules tend to promote new particles formation rather than particles growth. Note that these effects of NH_3 on particle initial growth might be more complex in the ambient air with high levels of SO_2, NH_3, NO_x, VOCs than current smog chamber experiments.

https://doi.org/10.5194/acp-2021-61
Preprint. Discussion started: 22 January 2021


Atmospheric Chemistry and Physics Discussions

3.2.2 Particle chemical composition in NH_3-involved photooxidation

The ATR-FTIR spectra of aerosol particles from NH_3-added experiment are also given in Fig. 5. A previous study suggested that the absorbances at 3310–3360 cm^{-1} and 1550–1650 cm^{-1} can be assigned to N-H stretch and C-N-H bend in secondary amine molecules, respectively (Babar et al., 2017). However, no evidence of secondary amine formation was detected and no clear FTIR spectra differences between aerosols from TMB/NO_x experiment and aerosols from TMB/NO_x/NH_3 photooxidation were found in this work (Fig. 5). It has been recently discovered that the conversion of oxidized organics to nitrogen-containing compounds in the presence of NH_3 is more likely to occur in high RH condition (Zhang et al., 2020). NH_3 uptake by TMB-derived aerosol particles may be limited to the aerosol surface under low RH condition (RH < 20%) (Bell et al., 2017). The amounts of secondary amine compounds formed from the NH_3 uptake by aerosol may be small, resulting in no characteristic peaks of secondary amine in ATR-FTIR spectra. Surprisingly, the effects of NH_3 on aerosol chemical compositions were increasingly important under SO_2-rich condition. As displayed in Fig. 5 (e), the strong C=O band at 1720 cm^{-1} converted to a shoulder upon NH_3 addition to the TMB/NO_x/SO_2 reaction system. In addition, the C-N stretch at 1332 cm^{-1} was observed in TMB/NO_x/SO_2/NH_3 photooxidation (Fig. 5). The particle-phase C-N stretch has been also characterized in m-xylene photooxidation experiments with NH_3 addition and was suggested to account for nitrogen-containing compounds (Liu et al., 2015). A smog chamber study also found that the coexistence of SO_2 and NH_3 substantially enhanced the formation of nitrogen-containing compounds from the photooxidation of toluene (Chu et al., 2016). In the current work, the presence of SO_2 could promote the increase in particle acidity. Elevating particle acidity could facilitate the reaction of NH_3/NH_4^+ with carbonyl-containing compounds, leading to the formation of nitrogen-containing organic compounds (Liu et al., 2015).

https://doi.org/10.5194/acp-2021-61
Preprint. Discussion started: 22 January 2021

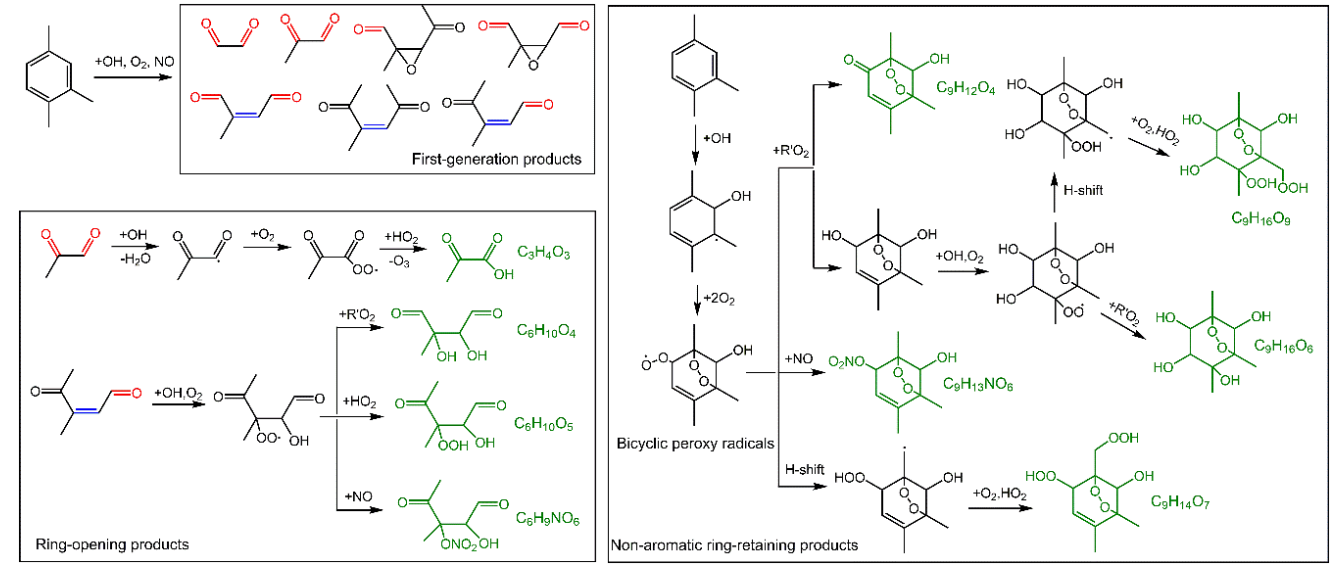

Figure 8. Simplified formation mechanism of the detected products in SOA formed from NH_3-involved photooxidation. Some observed products are produced through same chemical mechanism and for simplicity, only one product is drawn in this figure as an example.

The HRMS measurement results are consistent with FTIR analysis. As shown in the HRMS spectra of aerosol samples (Fig. S7), under SO_2-free condition, the presence of NH_3 did not result in considerable changes in peak numbers and abundance for both positive ion mode and negative ion mode. The major products (Table S3) are likely generated by similar chemical mechanisms (Fig. 8), which are not sensitive to the change in initial NH_3 levels under current experimental conditions. As depicted in Fig. 8, first, the photooxidation of TMB in the presence of NO can result in the formation of bicyclic oxy radicals that could decompose to a series of ring-opening products including biacetyl, epoxy-dicarbonyl, and carbonylic products (Li and Wang, 2014). These first-generation products could be further oxidized by OH. For example, oxidation of methylglyoxal by OH can proceed through abstraction of the aldehydic hydrogen to form the $CH_3C(O)C(O)\cdot$ radical, which may react with O_2 and then with HO_2 to form pyruvic acid. Second, bicyclic peroxy radicals (BPR) are key intermediates for the formation of non-aromatic ring-retaining products. Reactions of BPR with RO_2 can form either bicyclic carbonyl and bicyclic alcohol, which further undergoes OH oxidation to yield the $C_9H_{16}O_6$ and $C_9H_{16}O_9$ compounds. BPRs can produce bicyclic organonitrates by reaction with NO, and can also undergo intramolecular H-shift followed by O_2 addition to form a new bicyclic peroxy radical. The new bicyclic peroxy radical reacts with HO_2 to generate highly oxygenated organic molecules, consistent with a recent study (Wang et al., 2020b).

https://doi.org/10.5194/acp-2021-61
Preprint. Discussion started: 22 January 2021

Atmospheric Chemistry and Physics Discussions

To our knowledge, NH_3 does not basically affect the reaction of free radicals in gas-phase during the photooxidation of TMB. Generally, NH_3 levels play a negligible role in the aerosol organic composition in TMB photooxidation without SO_2 addition. In contrast, under SO_2-rich condition, the increase in NH_3 level led to a significant increase in the abundance of organic compounds (especially for compounds with m/z > 200) in both positive and negative ion modes (Fig. 9). The reaction of NH_3 with H_2SO_4 can form ammonium sulfate (Fig. S8), which is an attractive condensation sink for organic vapors and thus can increase the abundance of organic compounds in the bulk phase. To better explain this effect, the saturation mass concentrations of detected products were predicted based on a previous method (Li et al., 2016) and the calculated results are shown in Fig. 10 and Table S3. During the photooxidation of TMB, the fates of organic compounds are mainly governed by the competition between fragmentation and functionalization. Losing carbon atoms increases products volatility, which could be partly compensated by functionalization. Among the compounds present in aerosol particles formed from NH_3-added systems, fourteen products were C9 or smaller multifunctional oxidation products. The range of products saturation mass concentration spanned approximately 8 orders of magnitude, indicating that the measured particle-phase products are considerably different regarding volatility. From Fig. 10, the proposed products in the particle-phase are classified into three classes: low-volatility organic compound, intermediate volatility organic compounds, and semi-volatility organic compounds. The measured products might not be responsible for homogenous nucleation but these compounds can gradually condense onto nucleation particles (i.e., ammonium sulfate) to contribute to aerosol formation and growth, which highlights the role of ammonium sulfate in this case.

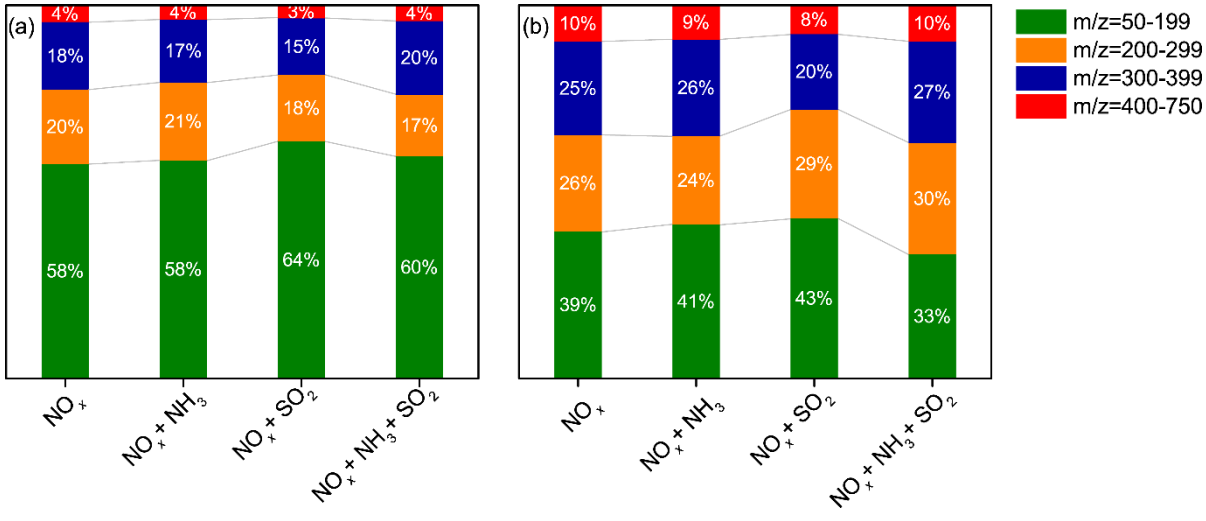

Figure 9. Relative contributions (% by abundance) of ions detected by UPLC-HRMS in the positive mode (a) and negative mode (b) for aerosol particles collected from different experiments (Exps. 5, 8, 10, 12).

https://doi.org/10.5194/acp-2021-61
Preprint. Discussion started: 22 January 2021

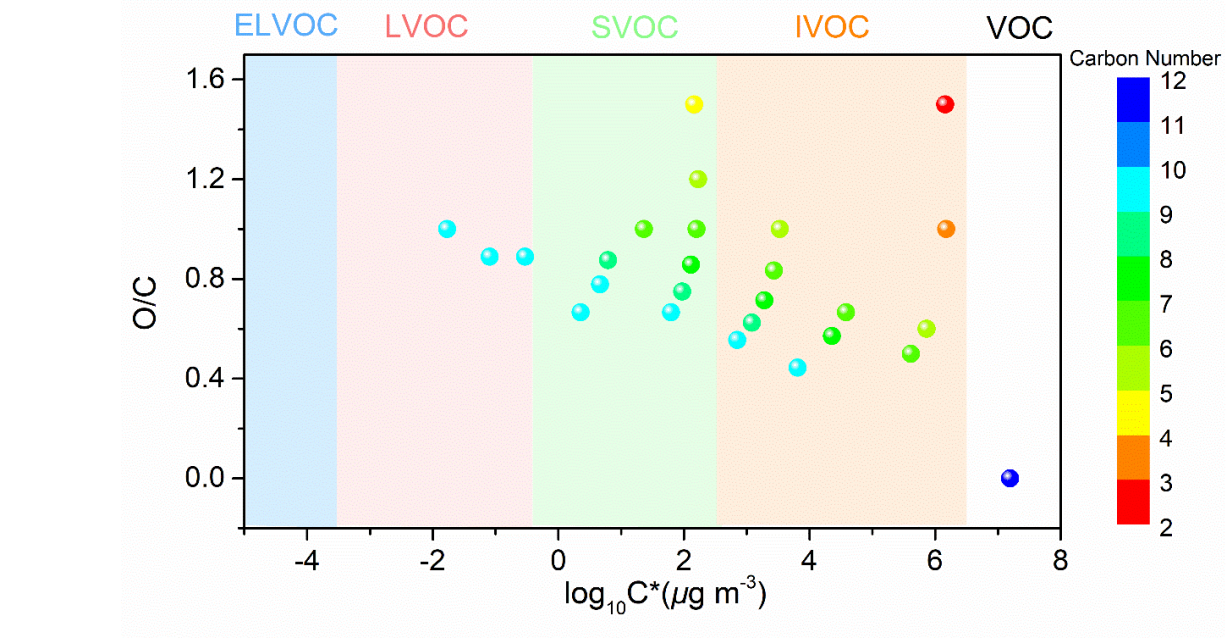

Figure 10. TMB and detected products displayed in the two-dimensional volatility-oxidation space (TMB/NO_x/NH_3 photooxidation). Based on the method of Li et al. (2016), we grouped the detected compounds in the classes of extremely low-volatility organic compound (ELVOC), low-volatility organic compound (LVOC), semi-volatility organic compound (SVOC), intermediate volatility organic compounds (IVOC), and volatility organic compound (VOC).

https://doi.org/10.5194/acp-2021-61
Preprint. Discussion started: 22 January 2021


Atmospheric Chemistry and Physics Discussions

4 Conclusions

In summary, we explored the detailed effects of SO_2 and NH_3 on secondary aerosol formation from TMB photooxidation. Our results demonstrate a substantial increase in ultrafine particle (< 100 nm) number concentrations resulting from SO_2 addition. Significant increases in SOA yields were found in TMB/NO_x/SO_2 photooxidation, due to acid-driven heterogeneous reaction that led to the formation of organosulfur compounds. The laboratory characterization of SOA composition confirmed the formation of new organosulfates at MW 214, 226, 228, 240, 242, 244, 268, 300, 316, and 345. The HRMS data give experimental evidence that the MW 214, 228, and 242 organosulfates could account for organosulfates previously designated as unknown origin in ambient $PM_{2.5}$, while some of them that were observed in TMB/NO_x/SO_2 photooxidation are isomers of recognized biogenic organosulfates. This indicates that care must be taken in the identification of TMB-derived organosulfates in ambient aerosols. More laboratory and field studies with organosulfate authentic standard should be carried out to determine the accurate yield of the measured organosulfates and the contribution of TMB-derived organosulfate to total atmospheric organosulfate. In addition, the composition of secondary aerosol could determine the physicochemical properties of aerosol particles (e.g. viscosity and phase state). Changes in SO_2 emissions in different regions all over the world have great implications for the physicochemical properties of aromatics-derived SOA and, thus, highly influence the global climate.

The presence of NH_3 also increased the number and volume concentration of secondary aerosol particles, especially under SO_2-rich condition. We characterized a series of multifunctional ring-retaining and ring-opening organic compounds containing one and even more carbonyl, alcohol, and nitrates groups. The predicted volatility distributions of products suggested that the measured later-generation products progressively condense onto nucleation particles to enhance particle formation in TMB/NO_x/NH_3 photooxidation. Current models that are used to assess aerosol-climate interactions should fully take into account the influence of NH_3 on secondary aerosol formation, which is especially significant in regions with strong NH_3 emissions.

https://doi.org/10.5194/acp-2021-61
Preprint. Discussion started: 22 January 2021

Atmospheric Chemistry and Physics Discussions

Data availability. Experimental data are available upon request to the corresponding author.

Supplement. The supplement related to this article is available online at:

Author contribution. Zhaomin Yang: Conceptualization, Methodology, Investigation, Validation, Visualization, Writing – original draft preparation. Li Xu: Investigation. Narcisse T. Tsona: Visualization, Writing – review & editing. Jianlong Li: Visualization, Writing – review & editing. Xin Luo: Methodology, Resources. Lin Du: Conceptualization, Investigation, Funding acquisition, Project administration, Resources, Supervision, Visualization, Writing – review & editing.

Competing interests. The authors declare that they have no conflict of interest.

Financial support. This work was supported by National Natural Science Foundation of China (91644214), Youth Innovation Program of Universities in Shandong Province (2019KJD007), and Fundamental Research Fund of Shandong University (2020QNQT012).

https://doi.org/10.5194/acp-2021-61
Preprint. Discussion started: 22 January 2021


Atmospheric Chemistry and Physics Discussions

References

Babar, Z. B., Park, J.-H., and Lim, H.-J.: Influence of NH_3 on secondary organic aerosols from the ozonolysis and photooxidation of α-pinene in a flow reactor, Atmos. Environ., 164, 71-84, 10.1016/j.atmosenv.2017.05.034, 2017.

Bell, D. M., Imre, D., S, T. M., and Zelenyuk, A.: The properties and behavior of alpha-pinene secondary organic aerosol particles exposed to ammonia under dry conditions, Phys. Chem. Chem. Phys., 19, 6497-6507, 10.1039/c6cp08839b, 2017.

Blair, S. L., MacMillan, A. C., Drozd, G. T., Goldstein, A. H., Chu, R. K., Pasa-Tolic, L., Shaw, J. B., Tolic, N., Lin, P., Laskin, J., Laskin, A., and Nizkorodov, S. A.: Molecular characterization of organosulfur compounds in biodiesel and diesel fuel secondary organic aerosol, Environ. Sci. Technol., 51, 119-127, 10.1021/acs.est.6b03304, 2017.

Boris, A. J., Lee, T., Park, T., Choi, J., Seo, S. J., and Collett Jr, J. L.: Fog composition at Baengnyeong Island in the eastern Yellow Sea: detecting markers of aqueous atmospheric oxidations, Atmos. Chem. Phys., 16, 437-453, 10.5194/acp-16-437-2016, 2016.

Cai, D., Wang, X., Chen, J., and Li, X.: Molecular characterization of organosulfates in highly polluted atmosphere using ultra-high-resolution mass spectrometry, J. Geophys. Res.-Atmos., 125, 10.1029/2019jd032253, 2020.

Chen, T., Liu, Y., Ma, Q., Chu, B., Zhang, P., Liu, C., Liu, J., and He, H.: Significant source of secondary aerosol: formation from gasoline evaporative emissions in the presence of SO_2 and NH_3, Atmos. Chem. Phys., 19, 8063-8081, 10.5194/acp-19-8063-2019, 2019.

Cheng, Y., Yu, Q.-Q., Liu, J.-M., Zhu, S., Zhang, M., Zhang, H., Zheng, B., and He, K.-B.: Model vs. observation discrepancy in aerosol characteristics during a half-year long campaign in Northeast China: The role of biomass burning, Environ. Pollut., 269, 116167-116167, 10.1016/j.envpol.2020.116167, 2021.

Chu, B., Zhang, X., Liu, Y., He, H., Sun, Y., Jiang, J., Li, J., and Hao, J.: Synergetic formation of secondary inorganic and organic aerosol: effect of SO_2 and NH_3 on particle formation and growth, Atmos. Chem. Phys., 16, 14219-14230, 2016.

Chu, B., Ma, Q., Liu, J., Ma, J., Zhang, P., Chen, T., Feng, Q., Wang, C., Yang, N., Ma, H., Ma, J., Russell, A. G., and He, H.: Air pollutant correlations in china: Secondary air pollutant responses to NO_x and SO_2 control, Environ. Sci. Technol. Lett., 7, 695-700, 10.1021/acs.estlett.0c00403, 2020.

Flores, J. M., Washenfelder, R. A., Adler, G., Lee, H. J., Segev, L., Laskin, J., Laskin, A., Nizkorodov, S. A., Brown, S. S., and Rudich, Y.: Complex refractive indices in the near-ultraviolet spectral region of biogenic secondary organic aerosol aged with ammonia, Phys. Chem. Chem. Phys., 16, 10629-10642, 10.1039/c4cp01009d, 2014.

Friedman, B., Brophy, P., Brune, W. H., and Farmer, D. K.: Anthropogenic Sulfur Perturbations on Biogenic Oxidation: SO_2 Additions Impact Gas-Phase OH Oxidation Products of α- and β-Pinene, Environ. Sci. Technol., 50, 1269-1279, 10.1021/acs.est.5b05010, 2016.

https://doi.org/10.5194/acp-2021-61
Preprint. Discussion started: 22 January 2021


Atmospheric Chemistry and Physics Discussions

Fu, X., Wang, S., Xing, J., Zhang, X., Wang, T., and Hao, J.: Increasing Ammonia Concentrations Reduce the Effectiveness of Particle Pollution Control Achieved via SO_2 and NO_x Emissions Reduction in East China, Environ. Sci. Technol. Lett., 4, 221-227, 10.1021/acs.estlett.7b00143, 2017.

Fuzzi, S., Baltensperger, U., Carslaw, K., Decesari, S., Denier van der Gon, H., Facchini, M. C., Fowler, D., Koren, I., Langford, B., Lohmann, U., Nemitz, E., Pandis, S., Riipinen, I., Rudich, Y., Schaap, M., Slowik, J. G., Spracklen, D. V., Vignati, E., Wild, M., Williams, M., and Gilardoni, S.: Particulate matter, air quality and climate: lessons learned and future needs, Atmos. Chem. Phys., 15, 8217-8299, 10.5194/acp-15-8217-2015, 2015.

Guo, H., Wang, T., Blake, D., Simpson, I., Kwok, Y., and Li, Y.: Regional and local contributions to ambient non-methane volatile organic compounds at a polluted rural/coastal site in Pearl River Delta, China, Atmos. Environ., 40, 2345-2359, 2006.

Guo, S., Hu, M., Zamora, M. L., Peng, J., Shang, D., Zheng, J., Du, Z., Wu, Z., Shao, M., Zeng, L., Molina, M. J., and Zhang, R.: Elucidating severe urban haze formation in China, P. Natl. Acad. Sci. USA, 111, 17373-17378, 10.1073/pnas.1419604111, 2014.

Hao, L., Kari, E., Leskinen, A., Worsnop, D. R., and Virtanen, A.: Direct contribution of ammonia to α-pinene secondary organic aerosol formation, Atmos. Chem. Phys., 20, 14393-14405, 10.5194/acp-20-14393-2020, 2020.

Heald, C. L., Kroll, J. H., Jimenez, J. L., Docherty, K. S., DeCarlo, P. F., Aiken, A. C., Chen, Q., Martin, S. T., Farmer, D. K., and Artaxo, P.: A simplified description of the evolution of organic aerosol composition in the atmosphere, Geophys. Res. Lett., 37, 10.1029/2010gl042737, 2010.

Henze, D. K., Seinfeld, J. H., Ng, N. L., Kroll, J. H., Fu, T. M., Jacob, D. J., and Heald, C. L.: Global modeling of secondary organic aerosol formation from aromatic hydrocarbons: high- vs. low-yield pathways, Atmos. Chem. Phys., 8, 2405-2420, 10.5194/acp-8-2405-2008, 2008.

Huang, R.-J., Zhang, Y., Bozzetti, C., Ho, K.-F., Cao, J.-J., Han, Y., Daellenbach, K. R., Slowik, J. G., Platt, S. M., Canonaco, F., Zotter, P., Wolf, R., Pieber, S. M., Bruns, E. A., Crippa, M., Ciarelli, G., Piazzalunga, A., Schwikowski, M., Abbaszade, G., Schnelle-Kreis, J., Zimmermann, R., An, Z., Szidat, S., Baltensperger, U., El Haddad, I., and Prevot, A. S. H.: High secondary aerosol contribution to particulate pollution during haze events in China, Nature, 514, 218-222, 10.1038/nature13774, 2014.

Jorga, S. D., Kaltsonoudis, C., Liangou, A., and Pandis, S. N.: Measurement of Formation Rates of Secondary Aerosol in the Ambient Urban Atmosphere Using a Dual Smog Chamber System, Environ. Sci. Technol., 54, 1336-1343, 10.1021/acs.est.9b03479, 2020.

Julin, J., Murphy, B. N., Patoulias, D., Fountoukis, C., Olenius, T., Pandis, S. N., and Riipinen, I.: Impacts of Future European Emission Reductions on Aerosol Particle Number Concentrations Accounting for Effects of Ammonia, Amines, and Organic Species, Environ. Sci. Technol., 52, 692-700, 10.1021/acs.est.7b05122, 2018.

Kanakidou, M., Seinfeld, J. H., Pandis, S. N., Barnes, I., Dentener, F. J., Facchini, M. C., Van Dingenen, R., Ervens, B., Nenes,

https://doi.org/10.5194/acp-2021-61
Preprint. Discussion started: 22 January 2021


Atmospheric Chemistry and Physics Discussions

A., Nielsen, C. J., Swietlicki, E., Putaud, J. P., Balkanski, Y., Fuzzi, S., Horth, J., Moortgat, G. K., Winterhalter, R., Myhre, C. E. L., Tsigaridis, K., Vignati, E., Stephanou, E. G., and Wilson, J.: Organic aerosol and global climate modelling: a review, Atmos. Chem. Phys., 5, 1053-1123, 10.5194/acp-5-1053-2005, 2005.

Kleindienst, T. E., Edney, E. O., Lewandowski, M., Offenberg, J. H., and Jaoui, M.: Secondary organic carbon and aerosol yields from the irradiations of isoprene and α-pinene in the presence of NO_x and SO_2, Environ. Sci. Technol., 40, 3807-3812, 10.1021/es052446r, 2006.

Kulmala, M., Petaja, T., Nieminen, T., Sipila, M., Manninen, H. E., Lehtipalo, K., Dal Maso, M., Aalto, P. P., Junninen, H., Paasonen, P., Riipinen, I., Lehtinen, K. E., Laaksonen, A., and Kerminen, V. M.: Measurement of the nucleation of atmospheric aerosol particles, Nat. Protoc., 7, 1651-1667, 10.1038/nprot.2012.091, 2012.

Lehtipalo, K., Yan, C., Dada, L., Bianchi, F., Xiao, M., Wagner, R., Stolzenburg, D., Ahonen, L. R., Amorim, A., Baccarini, A., Bauer, P. S., Baumgartner, B., Bergen, A., Bernhammer, A. K., Breitenlechner, M., Brilke, S., Buchholz, A., Mazon, S. B., Chen, D. X., Chen, X. M., Dias, A., Dommen, J., Draper, D. C., Duplissy, J., Ehn, M., Finkenzeller, H., Fischer, L., Frege, C., Fuchs, C., Garmash, O., Gordon, H., Hakala, J., He, X. C., Heikkinen, L., Heinritzi, M., Helm, J. C., Hofbauer, V., Hoyle, C. R., Jokinen, T., Kangasluoma, J., Kerminen, V. M., Kim, C., Kirkby, J., Kontkanen, J., Kurten, A., Lawler, M. J., Mai, H. J., Mathot, S., Mauldin, R. L., Molteni, U., Nichman, L., Nie, W., Nieminen, T., Ojdanic, A., Onnela, A., Passananti, M., Petaja, T., Piel, F., Pospisilova, V., Quelever, L. L. J., Rissanen, M. P., Rose, C., Sarnela, N., Schallhart, S., Schuchmann, S., Sengupta, K., Simon, M., Sipila, M., Tauber, C., Tome, A., Trostl, J., Vaisanen, O., Vogel, A. L., Volkamer, R., Wagner, A. C., Wang, M. Y., Weitz, L., Wimmer, D., Ye, P. L., Ylisirnio, A., Zha, Q. Z., Carslaw, K. S., Curtius, J., Donahue, N. M., Flagan, R. C., Hansel, A., Riipinen, I., Virtanen, A., Winkler, P. M., Baltensperger, U., Kulmala, M., and Worsnop, D. R.: Multicomponent new particle formation from sulfuric acid, ammonia, and biogenic vapors, Sci. Adv., 4, 9, 10.1126/sciadv.aau5363, 2018.

Lelieveld, J., Evans, J. S., Fnais, M., Giannadaki, D., and Pozzer, A.: The contribution of outdoor air pollution sources to premature mortality on a global scale, Nature, 525, 367-371, 10.1038/nature15371, 2015.

Li, K., Chen, L., White, S. J., Yu, H., Wu, X., Gao, X., Azzi, M., and Cen, K.: Smog chamber study of the role of NH3 in new particle formation from photo-oxidation of aromatic hydrocarbons, Sci. Total Environ., 619-620, 927-937, 10.1016/j.scitotenv.2017.11.180, 2018.

Li, Y., and Wang, L.: The atmospheric oxidation mechanism of 1,2,4-trimethylbenzene initiated by OH radicals, Phys. Chem. Chem. Phys., 16, 17908-17917, 10.1039/c4cp02027h, 2014.

Li, Y., Pöschl, U., and Shiraiwa, M.: Molecular corridors and parameterizations of volatility in the chemical evolution of organic aerosols, Atmos. Chem. Phys., 16, 3327-3344, 10.5194/acp-16-3327-2016, 2016.

Lin, Y. H., Knipping, E. M., Edgerton, E. S., Shaw, S. L., and Surratt, J. D.: Investigating the influences of SO_2 and NH_3 levels on isoprene-derived secondary organic aerosol formation using conditional sampling approaches, Atmos. Chem. Phys., 13,

https://doi.org/10.5194/acp-2021-61
Preprint. Discussion started: 22 January 2021


Atmospheric Chemistry and Physics Discussions

8457-8470, 10.5194/acp-13-8457-2013, 2013.

Liu, S., Shilling, J. E., Song, C., Hiranuma, N., Zaveri, R. A., and Russell, L. M.: Hydrolysis of Organonitrate Functional Groups in Aerosol Particles, Aerosol Sci. Technol., 46, 1359-1369, 10.1080/02786826.2012.716175, 2012.

Liu, S., Jia, L., Xu, Y., Tsona, N. T., Ge, S., and Du, L.: Photooxidation of cyclohexene in the presence of SO_2: SOA yield and chemical composition, Atmos. Chem. Phys., 17, 13329-13343, 10.5194/acp-17-13329-2017, 2017.

Liu, T., Wang, X., Hu, Q., Deng, W., Zhang, Y., Ding, X., Fu, X., Bernard, F., Zhang, Z., Lu, S., He, Q., Bi, X., Chen, J., Sun, Y., Yu, J., Peng, P., Sheng, G., and Fu, J.: Formation of secondary aerosols from gasoline vehicle exhaust when mixing with SO_2, Atmos. Chem. Phys., 16, 675-689, 10.5194/acp-16-675-2016, 2016.

Liu, Y., Liggio, J., Staebler, R., and Li, S. M.: Reactive uptake of ammonia to secondary organic aerosols: kinetics of organonitrogen formation, Atmos. Chem. Phys., 15, 13569-13584, 10.5194/acp-15-13569-2015, 2015.

Lu, X., and Zhang, Y.: Volatility of Ammonium Nitrate in Ultra-viscous Aerosol Droplets by Optical Tweezers, Acta Chimi. Sin., 78, 326-329, 10.6023/a19100369, 2020.

Ma, Y., Xu, X., Song, W., Geng, F., and Wang, L.: Seasonal and diurnal variations of particulate organosulfates in urban Shanghai, China, Atmos. Environ., 85, 152-160, 10.1016/j.atmosenv.2013.12.017, 2014.

Mehra, A., Wang, Y., Krechmer, J. E., Lambe, A., Majluf, F., Morris, M. A., Priestley, M., Bannan, T. J., Bryant, D. J., Pereira, K. L., Hamilton, J. F., Rickard, A. R., Newland, M. J., Stark, H., Croteau, P., Jayne, J. T., Worsnop, D. R., Canagaratna, M. R., Wang, L., and Coe, H.: Evaluation of the chemical composition of gas- and particle-phase products of aromatic oxidation, Atmos. Chem. Phys., 20, 9783-9803, 10.5194/acp-20-9783-2020, 2020.

Mo, Z., Lu, S., and Shao, M.: Volatile organic compound (VOC) emissions and health risk assessment in paint and coatings industry in the Yangtze River Delta, China, Environ. Pollut., 269, 115740, 10.1016/j.envpol.2020.115740, 2021.

Na, K., Song, C., and Cockeriii, D.: Formation of secondary organic aerosol from the reaction of styrene with ozone in the presence and absence of ammonia and water, Atmos. Environ., 40, 1889-1900, 10.1016/j.atmosenv.2005.10.063, 2006.

Na, K., Song, C., Switzer, C., and Cocker, D. R., III: Effect of ammonia on secondary organic aerosol formation from alpha-Pinene ozonolysis in dry and humid conditions, Environ. Sci. Technol., 41, 6096-6102, 10.1021/es061956y, 2007.

Nestorowicz, K., Jaoui, M., Rudzinski, K. J., Lewandowski, M., Kleindienst, T. E., Spolnik, G., Danikiewicz, W., and Szmigielski, R.: Chemical composition of isoprene SOA under acidic and non-acidic conditions: effect of relative humidity, Atmos. Chem. Phys., 18, 18101-18121, 10.5194/acp-18-18101-2018, 2018.

Ng, N. L., Kroll, J. H., Chan, A. W. H., Chhabra, P. S., Flagan, R. C., and Seinfeld, J. H.: Secondary organic aerosol formation from m-xylene, toluene, and benzene, Atmos. Chem. Phys., 7, 3909-3922, 10.5194/acp-7-3909-2007, 2007.

O'Brien, R. E., Laskin, A., Laskin, J., Rubitschun, C. L., Surratt, J. D., and Goldstein, A. H.: Molecular characterization of S- and N-containing organic constituents in ambient aerosols by negative ion mode high-resolution Nanospray Desorption

https://doi.org/10.5194/acp-2021-61
Preprint. Discussion started: 22 January 2021


Atmospheric Chemistry and Physics Discussions

675 Electrospray Ionization Mass Spectrometry: CalNex 2010 field study, J. Geophys. Res. Atmos., 119, 12706-12720, 10.1002/2014jd021955, 2014.

Odum, J. R., Hoffmann, T., Bowman, F., Collins, D., Flagan, R. C., and Seinfeld, J. H.: Gas/particle partitioning and secondary organic aerosol yields, Environ. Sci. Technol., 30, 2580-2585, 10.1021/es950943+, 1996.

Ran, L., Zhao, C., Geng, F., Tie, X., Tang, X., Peng, L., Zhou, G., Yu, Q., Xu, J., and Guenther, A.: Ozone photochemical
680 production in urban Shanghai, China: Analysis based on ground level observations, J. Geophys. Res. Atmos., 114, 10.1029/2008jd010752, 2009.

Riva, M., Tomaz, S., Cui, T., Lin, Y.-H., Perraudin, E., Gold, A., Stone, E. A., Villenave, E., and Surratt, J. D.: Evidence for an Unrecognized Secondary Anthropogenic Source of Organosulfates and Sulfonates: Gas-Phase Oxidation of Polycyclic Aromatic Hydrocarbons in the Presence of Sulfate Aerosol, Environ. Sci. Technol., 49, 6654-6664, 10.1021/acs.est.5b00836,
685 2015a.

Riva, M., Tomaz, S., Cui, T. Q., Lin, Y. H., Perraudin, E., Gold, A., Stone, E. A., Villenave, E., and Surratt, J. D.: Evidence for an unrecognized secondary anthropogenic source of organosulfates and sulfonates: gas-phase oxidation of polycyclic aromatic hydrocarbons in the presence of sulfate aerosol, Environ. Sci. Technol., 49, 6654-6664, 10.1021/acs.est.5b00836, 2015b.

Riva, M., Barbosa, T. D. S., Lin, Y.-H., Stone, E. A., Gold, A., and Surratt, J. D.: Chemical characterization of organosulfates
690 in secondary organic aerosol derived from the photooxidation of alkanes, Atmos. Chem. Phys., 16, 11001-11018, 10.5194/acp-16-11001-2016, 2016a.

Riva, M., Budisulistiorini, S. H., Chen, Y., Zhang, Z., D'Ambro, E. L., Zhang, X., Gold, A., Turpin, B. J., Thornton, J. A., Canagaratna, M. R., and Surratt, J. D.: Chemical Characterization of Secondary Organic Aerosol from Oxidation of Isoprene Hydroxyhydroperoxides, Environ. Sci. Technol., 50, 9889-9899, 10.1021/acs.est.6b02511, 2016b.

695 Riva, M., Chen, Y., Zhang, Y., Lei, Z., Olson, N. E., Boyer, H. C., Narayan, S., Yee, L. D., Green, H. S., Cui, T., Zhang, Z., Baumann, K., Fort, M., Edgerton, E., Budisulistiorini, S. H., Rose, C. A., Ribeiro, I. O., RL, E. O., Dos Santos, E. O., Machado, C. M. D., Szopa, S., Zhao, Y., Alves, E. G., de Sa, S. S., Hu, W., Knipping, E. M., Shaw, S. L., Duvoisin Junior, S., de Souza, R. A. F., Palm, B. B., Jimenez, J. L., Glasius, M., Goldstein, A. H., Pye, H. O. T., Gold, A., Turpin, B. J., Vizuete, W., Martin, S. T., Thornton, J. A., Dutcher, C. S., Ault, A. P., and Surratt, J. D.: Increasing Isoprene Epoxydiol-to-Inorganic Sulfate Aerosol
700 Ratio Results in Extensive Conversion of Inorganic Sulfate to Organosulfur Forms: Implications for Aerosol Physicochemical Properties, Environ. Sci. Technol., 53, 8682-8694, 10.1021/acs.est.9b01019, 2019.

Sarrafzadeh, M., Wildt, J., Pullinen, I., Springer, M., Kleist, E., Tillmann, R., Schmitt, S. H., Wu, C., Mentel, T. F., Zhao, D., Hastie, D. R., and Kiendler-Scharr, A.: Impact of NO_x and OH on secondary organic aerosol formation from β-pinene photooxidation, Atmos. Chem. Phys., 16, 11237-11248, 10.5194/acp-16-11237-2016, 2016.

705 Shalamzari, M. S., Kahnt, A., Vermeylen, R., Kleindienst, T. E., Lewandowski, M., Cuyckens, F., Maenhaut, W., and Claeys,

https://doi.org/10.5194/acp-2021-61
Preprint. Discussion started: 22 January 2021


Atmospheric Chemistry and Physics Discussions

M.: Characterization of polar organosulfates in secondary organic aerosol from the green leaf volatile 3-Z-hexenal, Environ. Sci. Technol., 48, 12671-12678, 10.1021/es503226b, 2014.

Shrivastava, M., Fast, J., Easter, R., Gustafson, W. I., Zaveri, R. A., Jimenez, J. L., Saide, P., and Hodzic, A.: Modeling organic aerosols in a megacity: comparison of simple and complex representations of the volatility basis set approach, Atmos. Chem. Phys., 11, 6639-6662, 10.5194/acp-11-6639-2011, 2011.

Shrivastava, M., Cappa, C. D., Fan, J., Goldstein, A. H., Guenther, A. B., Jimenez, J. L., Kuang, C., Laskin, A., Martin, S. T., Ng, N. L., Petaja, T., Pierce, J. R., Rasch, P. J., Roldin, P., Seinfeld, J. H., Shilling, J., Smith, J. N., Thornton, J. A., Volkamer, R., Wang, J., Worsnop, D. R., Zaveri, R. A., Zelenyuk, A., and Zhang, Q.: Recent advances in understanding secondary organic aerosol: Implications for global climate forcing, Rev. Geophys., 55, 509-559, 10.1002/2016rg000540, 2017.

Song, C., Wu, L., Xie, Y., He, J., Chen, X., Wang, T., Lin, Y., Jin, T., Wang, A., Liu, Y., Dai, Q., Liu, B., Wang, Y. N., and Mao, H.: Air pollution in China: Status and spatiotemporal variations, Environ. Pollut., 227, 334-347, 10.1016/j.envpol.2017.04.075, 2017.

Surratt, J. D., Gomez-Gonzalez, Y., Chan, A. W. H., Vermeylen, R., Shahgholi, M., Kleindienst, T. E., Edney, E. O., Offenberg, J. H., Lewandowski, M., Jaoui, M., Maenhaut, W., Claeys, M., Flagan, R. C., and Seinfeld, J. H.: Organosulfate formation in biogenic secondary organic aerosol, J. Phys. Chem. A, 112, 8345-8378, 10.1021/jp802310p, 2008.

Terzano, C., Di Stefano, F., Conti, V., Graziani, E., and Petroianni, A.: Air pollution ultrafine particles: toxicity beyond the lung, Eur. Rev. Med. Pharmacol. Sci., 14, 809-821, 2010.

Tolocka, M. P., and Turpin, B.: Contribution of organosulfur compounds to organic aerosol mass, Environ. Sci. Technol., 46, 7978-7983, 10.1021/es300651v, 2012.

Volkamer, R., Jimenez, J. L., San Martini, F., Dzepina, K., Zhang, Q., Salcedo, D., Molina, L. T., Worsnop, D. R., and Molina, M. J.: Secondary organic aerosol formation from anthropogenic air pollution: Rapid and higher than expected, Geophys. Res. Lett., 33, 10.1029/2006gl026899, 2006.

Wang, M., Kong, W., Marten, R., He, X. C., Chen, D., Pfeifer, J., Heitto, A., Kontkanen, J., Dada, L., Kurten, A., Yli-Juuti, T., Manninen, H. E., Amanatidis, S., Amorim, A., Baalbaki, R., Baccarini, A., Bell, D. M., Bertozzi, B., Brakling, S., Brilke, S., Murillo, L. C., Chiu, R., Chu, B., De Menezes, L. P., Duplissy, J., Finkenzeller, H., Carracedo, L. G., Granzin, M., Guida, R., Hansel, A., Hofbauer, V., Krechmer, J., Lehtipalo, K., Lamkaddam, H., Lampimaki, M., Lee, C. P., Makhmutov, V., Marie, G., Mathot, S., Mauldin, R. L., Mentler, B., Muller, T., Onnela, A., Partoll, E., Petaja, T., Philippov, M., Pospisilova, V., Ranjithkumar, A., Rissanen, M., Rorup, B., Scholz, W., Shen, J., Simon, M., Sipila, M., Steiner, G., Stolzenburg, D., Tham, Y. J., Tome, A., Wagner, A. C., Wang, D. S., Wang, Y., Weber, S. K., Winkler, P. M., Wlasits, P. J., Wu, Y., Xiao, M., Ye, Q., Zauner-Wieczorek, M., Zhou, X., Volkamer, R., Riipinen, I., Dommen, J., Curtius, J., Baltensperger, U., Kulmala, M., Worsnop, D. R., Kirkby, J., Seinfeld, J. H., El-Haddad, I., Flagan, R. C., and Donahue, N. M.: Rapid growth of new atmospheric particles

https://doi.org/10.5194/acp-2021-61
Preprint. Discussion started: 22 January 2021


Atmospheric Chemistry and Physics Discussions

by nitric acid and ammonia condensation, Nature, 581, 184-189, 10.1038/s41586-020-2270-4, 2020a.

Wang, S., Zhou, S., Tao, Y., Tsui, W. G., Ye, J., Yu, J. Z., Murphy, J. G., McNeill, V. F., Abbatt, J. P. D., and Chan, A. W. H.: Organic Peroxides and Sulfur Dioxide in Aerosol: Source of Particulate Sulfate, Environ. Sci. Technol., 53, 10695-10704, 10.1021/acs.est.9b02591, 2019a.

Wang, X. K., Rossignol, S., Ma, Y., Yao, L., Wang, M. Y., Chen, J. M., George, C., and Wang, L.: Molecular characterization of atmospheric particulate organosulfates in three megacities at the middle and lower reaches of the Yangtze River, Atmos. Chem. Phys., 16, 2285-2298, 10.5194/acp-16-2285-2016, 2016.

Wang, Y., Ma, Y., Li, X., Kuang, B. Y., Huang, C., Tong, R., and Yu, J. Z.: Monoterpene and Sesquiterpene alpha-Hydroxy Organosulfates: Synthesis, MS/MS Characteristics, and Ambient Presence, Environ. Sci. Technol., 53, 12278-12290, 10.1021/acs.est.9b04703, 2019b.

Wang, Y., Mehra, A., Krechmer, J. E., Yang, G., Hu, X., Lu, Y., Lambe, A., Canagaratna, M., Chen, J., Worsnop, D., Coe, H., and Wang, L.: Oxygenated products formed from OH-initiated reactions of trimethylbenzene: autoxidation and accretion, Atmos. Chem. Phys., 20, 9563-9579, 10.5194/acp-20-9563-2020, 2020b.

Warner, J. X., Dickerson, R. R., Wei, Z., Strow, L. L., Wang, Y., and Liang, Q.: Increased atmospheric ammonia over the world's major agricultural areas detected from space, Geophys. Res. Lett., 44, 2875-2884, 10.1002/2016gl072305, 2017.

Wu, Y., Gu, B., Erisman, J. W., Reis, S., Fang, Y., Lu, X., and Zhang, X.: $PM_{2.5}$ pollution is substantially affected by ammonia emissions in China, Environ. Pollut., 218, 86-94, 10.1016/j.envpol.2016.08.027, 2016.

Wyche, K. P., Monks, P. S., Ellis, A. M., Cordell, R. L., Parker, A. E., Whyte, C., Metzger, A., Dommen, J., Duplissy, J., Prevot, A. S. H., Baltensperger, U., Rickard, A. R., and Wulfert, F.: Gas phase precursors to anthropogenic secondary organic aerosol: detailed observations of 1,3,5-trimethylbenzene photooxidation, Atmos. Chem. Phys., 9, 635-665, 10.5194/acp-9-635-2009, 2009.

Xu, L., Guo, H., Boyd, C. M., Klein, M., Bougiatioti, A., Cerully, K. M., Hite, J. R., Isaacman-VanWertz, G., Kreisberg, N. M., Knote, C., Olson, K., Koss, A., Goldstein, A. H., Hering, S. V., de Gouw, J., Baumann, K., Lee, S.-H., Nenes, A., Weber, R. J., and Ng, N. L.: Effects of anthropogenic emissions on aerosol formation from isoprene and monoterpenes in the southeastern United States, P. Natl Acad. Sci. U. S. A, 112, 37-42, 10.1073/pnas.1417609112, 2015.

Yang, Z., Tsona, N. T., Li, J., Wang, S., Xu, L., You, B., and Du, L.: Effects of NO_x and SO_2 on the secondary organic aerosol formation from the photooxidation of 1,3,5-trimethylbenzene: A new source of organosulfates, Environ. Pollut., 264, 114742, 10.1016/j.envpol.2020.114742, 2020.

Ye, J., Abbatt, J. P. D., and Chan, A. W. H.: Novel pathway of SO_2 oxidation in the atmosphere: reactions with monoterpene ozonolysis intermediates and secondary organic aerosol, Atmos. Chem. Phys., 18, 5549-5565, 10.5194/acp-18-5549-2018, 2018.

https://doi.org/10.5194/acp-2021-61
Preprint. Discussion started: 22 January 2021


Atmospheric Chemistry and Physics Discussions

Yu, Z., and Jang, M.: Atmospheric Processes of Aromatic Hydrocarbons in the Presence of Mineral Dust Particles in an Urban Environment, ACS Earth Space Chem., 3, 2404-2414, 10.1021/acsearthspacechem.9b00195, 2019.

Zaytsev, A., Koss, A. R., Breitenlechner, M., Krechmer, J. E., Nihill, K. J., Lim, C. Y., Rowe, J. C., Cox, J. L., Moss, J., Roscioli, J. R., Canagaratna, M. R., Worsnop, D., Kroll, J. H., and Keutsch, F. N.: Mechanistic study of the formation of ring-retaining and ring-opening products from the oxidation of aromatic compounds under urban atmospheric conditions, Atmos. Chem. Phys., 19, 15117-15129, 10.5194/acp-19-15117-2019, 2019.

Zhang, G., Lian, X., Fu, Y., Lin, Q., Li, L., Song, W., Wang, Z., Tang, M., Chen, D., Bi, X., Wang, X., and Sheng, G.: High secondary formation of nitrogen-containing organics (NOCs) and its possible link to oxidized organics and ammonium, Atmos. Chem. Phys., 20, 1469-1481, 10.5194/acp-20-1469-2020, 2020.

Zhang, R., Wang, G., Guo, S., Zamora, M. L., Ying, Q., Lin, Y., Wang, W., Hu, M., and Wang, Y.: Formation of urban fine particulate matter, Chem. Rev., 115, 3803-3855, 10.1021/acs.chemrev.5b00067, 2015.

Zhang, X., Cappa, C. D., Jathar, S. H., McVay, R. C., Ensber, J. J., Kleeman, M. J., and Seinfeld, J. H.: Influence of vapor wall loss in laboratory chambers on yields of secondary organic aerosol, P. Natl. Acad. Sci. USA, 111, 5802-5807, 2014.

Zhao, D., Schmitt, S. H., Wang, M., Acir, I.-H., Tillmann, R., Tan, Z., Novelli, A., Fuchs, H., Pullinen, I., Wegener, R., Rohrer, F., Wildt, J., Kiendler-Scharr, A., Wahner, A., and Mentel, T. F.: Effects of NO_x and SO_2 on the secondary organic aerosol formation from photooxidation of α-pinene and limonene, Atmos. Chem. Phys., 18, 1611-1628, 10.5194/acp-18-1611-2018, 2018.

Zhu, Y., Sabaliauskas, K., Liu, X., Meng, H., Gao, H., Jeong, C.-H., Evans, G. J., and Yao, X.: Comparative analysis of new particle formation events in less and severely polluted urban atmosphere, Atmos. Environ., 98, 655-664, 10.1016/j.atmosenv.2014.09.043, 2014.

Ziemann, P. J., and Atkinson, R.: Kinetics, products, and mechanisms of secondary organic aerosol formation, Chem. Soc. Rev., 41, 6582-6605, 10.1039/c2cs35122f, 2012.

Zou, Y., Deng, X. J., Zhu, D., Gong, D. C., Wang, H., Li, F., Tan, H. B., Deng, T., Mai, B. R., Liu, X. T., and Wang, B. G.: Characteristics of 1 year of observational data of VOCs, NO_x and O_3 at a suburban site in Guangzhou, China, Atmos. Chem. Phys., 15, 6625-6636, 10.5194/acp-15-6625-2015, 2015.